Chapter 8
A Few Notions of Stability and Bifurcation Theory

While numerical approaches are a very important step in investigating the patterns exhibited by the hyperbolic and kinetic models discussed in the previous chapters, they could be slow and might not offer a full understanding of the models' dynamics due to the very large parameter space associated with some models. Moreover, the analytical approaches discussed in Chap. 2 could offer an understanding of the parameter space where different types of solutions could occur (e.g., finite vs. density-blow up solutions, shocks vs. rarefaction waves, etc.). However, they cannot offer much insight into the conditions for the formation of patterns, as well as the transitions between different patterns.

Stability theory could identify the parameter conditions under which a pattern could form, and eventually could become unstable giving rise to a different pattern. While linear and weakly-linear stability analyses of homogeneous steady states are relatively easy tasks, stability analysis of spatially heterogeneous solutions is complicated by the complexity of the hyperbolic and kinetic models discussed throughout this monograph, and in particular the nonlinear and nonlocal structure of some of these models. Also difficult is the fully nonlinear stability analysis, which is often specific to the system being investigated [1]. As already mentioned, the nonlocality of the models presented in this monograph complicates the analysis even more—which explains the lack of studies focused on the nonlinear analysis of nonlocal (hyperbolic and kinetic) models for collective dynamics in biological aggregations.

A deeper understanding of the formation of various spatial and spatio-temporal patterns is offered by the bifurcation theory, which can distil the mathematical and biological mechanisms not only behind the formation of patterns, but also behind the transitions between different spatial and spatio-temporal patterns. In the following, we will review some basic notions of linear stability analysis for pattern formation in partial differential equations, as well as basic notions of symmetry theory and bifurcation theory. These will help the reader understand better the approaches taken by some of the studies reviewed in Chaps. 3–6. For more detailed discussions of

R. Eftimie, *Hyperbolic and Kinetic Models for Self-organised Biological Aggregations*, Lecture Notes in Mathematics 2232,
https://doi.org/10.1007/978-3-030-02586-1_8

these topics in stability and bifurcation theory, we refer the reader to the books by Hoyle [2], Golubitsky and Stewart [3], Chossat and Lauterbach [4], Haragus and Iooss [5], Kuznetsov [6], and Strogatz [7].

8.1 Basic Notions of Linear Stability Analysis

The first step in the investigation of pattern formation, is the identification of steady states (spatially homogeneous and, if possible, spatially heterogeneous) and their stability—since unstable states are usually associated with pattern formation and transitions between different patterns. The linear stability technique involves the identification of the eigenvalues of the linearised equation/system at the equilibrium (steady state) points, with the goal of understanding the quantitative behaviour of the solution near these points

We start the discussion of linear stability analysis by focusing first on ODEs, and then on PDEs. Since the majority of studies in the mathematical literature exemplify the linear stability analysis by focusing on parabolic reaction-diffusion equations [8], here we decided to change a bit the approach and to focus on nonlocal hyperbolic systems. This is particularly relevant in the context of the models discussed throughout the previous chapters.

8.1.1 Linear Stability Analysis for ODE Models

Consider the following ODE model

$$\frac{du}{dt} = f(u), \quad \text{with } u, f \in \mathbb{R}^n. \tag{8.1}$$

The dynamics of this system is controlled, in the long term, by the *steady states* (or *fixed points* or *equilibrium points*) of the system. A *steady state* of system (8.1) is a time-independent solution $u(t) = u^*$ that satisfies $f(u^*) = 0$.

To investigate the linear stability of these steady states u^*, we consider small temporal perturbations: $u(t) = u^* + ae^{\lambda t}$. After substituting these expressions back into (8.1) and linearising the nonlinear terms $f(u)$ about the steady states, we obtain that the linear stability of these states is controlled by the eigenvalues of the Jacobian matrix J:

$$J(u^*) = D_u f(u^*) = \begin{pmatrix} \frac{\partial f_1}{\partial u_1} & \cdots & \frac{\partial f_1}{\partial u_n} \\ \cdots & \cdots & \cdots \\ \frac{\partial f_n}{\partial u_n} & \cdots & \frac{\partial f_n}{\partial u_n} \end{pmatrix}_{u=u^*}$$
$$\text{for } f = (f_1, \ldots, f_n),\ u = (u_1, \ldots, u_n). \tag{8.2}$$

If all eigenvalues λ of the characteristic equation $\det(J(u) - \lambda I) = 0$ have negative real parts, we say that the steady state is linearly stable. If there are eigenvalues with positive real parts we say that the steady state is unstable.

For a system in $\mathbb{R}^2$ one can classify the fixed points in terms of the determinant $\det(J) = \lambda_1\lambda_2$ and trace $Tr(J) = \lambda_1 + \lambda_2$ of the Jacobian matrix (where λ_1 and λ_2 are the two eigenvalues). For example, if $\det(J) < 0$, the eigenvalues are real and of opposite signs and the fixed point is a saddle point. If $\det(J) > 0$ the eigenvalues are either real and of opposite signs (and thus they are nodes) or complex conjugates (and thus they are spirals or centres). If $\det(J) = 0$, at least one eigenvalue is zero. The stability of the nodes and spirals is given by $Tr(J)$: the fixed points are stable for $Tr(J) < 0$, and unstable for $Tr(J) > 0$. When $Tr(J) = 0$ the eigenvalues are purely imaginary, and the fixed points are centres. For more details on this fixed point classification, see [7, 9].

Definition 8.1 A fixed point u^* of (8.1) is called *hyperbolic* if and only if the Jacobian matrix $J(u^*)$ does not have any eigenvalues with zero real parts, i.e., $Re(\lambda_i) \neq 0$ for $i = 1, 2, \ldots, n$.

The stability of hyperbolic fixed points is not affected by small perturbations caused by nonlinear small terms (the local phase portrait near a hyperbolic fixed point being topologically equivalent to the phase portrait of the linearised system—see the Hartman-Grobman theorem in [9, 10]). In regard to pattern formation, the important cases are those where the eigenvalues have zero real parts ($Re(\lambda) = 0$), i.e., the fixed points are *non-hyperbolic*. The changes in the stability of fixed points, which suggest the possibility of a bifurcation, can only happen at non-hyperbolic fixed points. To conclude this section, we note that the qualitative behaviour of system (8.1) in the neighborhood of a nonhyperbolic fixed point u^* is determined by its behaviour on the centre manifold near u^*. Moreover, since the dimension of the centre manifold is usually smaller than the dimension of the full system (8.1), it becomes easier to investigate the qualitative behaviour of the system near a nonhyperbolic fixed point. We will return to the discussion of the centre manifold theory in Sect. 8.6. For a more comprehensive study on the stability of fixed points of ODE systems, we refer the reader to [9].

8.1.2 Linear Stability Analysis for PDE Models

Let us focus now on partial differential equations (PDEs), and assume that the models described in the previous chapters can be written in a general form as

$$\frac{\partial u(\mathbf{x}, t)}{\partial t} = \mathscr{L}[u(\mathbf{x}, t)] + \mathscr{N}[u(\mathbf{x}, t)], \quad (\mathbf{x}, t) \in \mathbb{R}^d \times \mathbb{R}^1_+, \tag{8.3}$$

where $\mathscr{L}[u]$ is a linear operator and $\mathscr{N}[u]$ is a nonlinear operator (containing higher order terms $O(u^k)$, $k \geq 2$, both local and nonlocal). Note that we have used $[\cdot]$

instead of $(\cdot)$ to emphasise that these linear and nonlinear terms can depend also nonlocally on $u(\mathbf{x}, t)$.

Definition 8.2 A *spatially homogeneous steady state* of (8.3) is a solution $u(\mathbf{x}, t) = u^* =$constant which satisfies

$$0 = \mathscr{L}[u^*] + \mathscr{N}[u^*]. \tag{8.4}$$

A *spatially heterogeneous steady state* of (8.3) is a solution $u(\mathbf{x}, t) = u^{**}(\mathbf{x})$ which satisfies

$$0 = \mathscr{L}[u^{**}(\mathbf{x})] + \mathscr{N}[u^{**}(\mathbf{x})]. \tag{8.5}$$

We characterise a steady state as being stable or unstable if small perturbations of this steady state decay or grow. Since a large part of this monograph focuses on nonlocal hyperbolic systems, to exemplify the linear stability technique, we focus on a generic 1D nonlocal hyperbolic system

$$\frac{\partial u^+}{\partial t} + \gamma \frac{\partial u^+}{\partial x} = -\lambda^+[u^+, u^-]u^+ + \lambda^-[u^+, u^-]u^-, \tag{8.6a}$$

$$\frac{\partial u^-}{\partial t} - \gamma \frac{\partial u^-}{\partial x} = \lambda^+[u^+, u^-]u^+ - \lambda^-[u^+, u^-]u^-, \tag{8.6b}$$

on a finite domain $[0, L]$ with periodic boundary conditions, and investigate the linear stability of a generic spatially homogeneous steady state $(u^+(t, x), u^-(t, x)) = (u^*_+, u^*_-)$. For example, the class of nonlocal hyperbolic systems (8.6) with the five communication mechanisms M1–M5 (see Table 5.1) introduced in [11] can exhibit one, three or five steady states; see Fig. 8.1a.

In the following we focus on the linear stability of a generic spatially homogeneous steady state (u^+_*, u^-_*)—any one of the states depicted in Fig. 8.1. (For a detailed discussion of the linear stability approach in reaction diffusion systems, i.e., Turing mechanisms, see [8].) We note that the stability of a spatially heterogeneous steady state $(u^{**}_+(x), u^{**}_-(x))$ follows the same approach, but the calculations are more challenging; see, for example, the studies in [12, 13] in the context of local parabolic equations; to our knowledge, studies on the stability of heterogeneous states exhibited by nonlocal hyperbolic equations/systems are very scarce, due to the challenge posed by dealing with the nonlocal terms. Also challenging is the application of nonlinear stability methods, which can offer more information about the formation of patterns, compared to the classical linear methods [1].

We start the linear stability analysis of a steady state (u^+_*, u^-_*) of system (8.6) by considering small-amplitude perturbations of the steady state: $u^+(x, t) = u^*_+ + v^+(x, t)$ and $u^-(x, t) = u^*_- + v^-(x, t)$ with $v^\pm(x, t) \propto a_\pm e^{\sigma t + ikx}$ and $|a_\pm| \ll 1$. Here $\sigma \in \mathbb{C}$ is an eigenvalue that gives the temporal growth/decay of the small perturbations (if $Re(\sigma) > 0$ or $Re(\sigma) < 0$, respectively), and k is the wavenumber (which is a measure of the wavelike pattern, being proportional to the reciprocal of

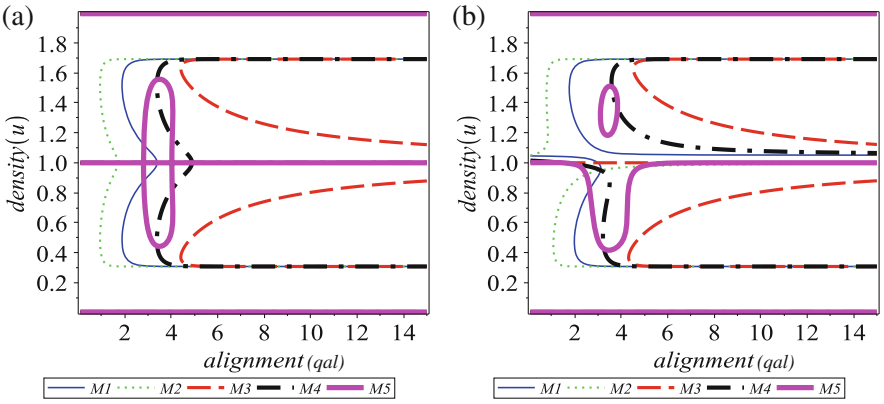

Fig. 8.1 Plot of steady state u_*^+ corresponding to (u_*^+, u_*^-)=$(u_*^+, A - u_*^+)$, as a function of the magnitude of alignment parameter q_{al}, for the five communication models introduced in [11]. In the expression of the steady states, we have $A = \frac{1}{L}\int_0^L (u^+(x) + u^-(x))dx$ the total population density on a finite domain $[0, L]$. We compare the cases of (**a**) *symmetric perception* of neighbours, versus (**b**) *asymmetric perception* of neighbours, as described by Eq. (5.20) and Fig. 5.6. In (**a**) we have $p_+ = p_- = 1.0$ (corresponding to symmetric perception), while in (**b**) we have $p_+ = 1.05$ and $p_- = 0.95$ (corresponding to asymmetric perception)

the wavelength ω of the pattern: $k = 2\pi/\omega$). For finite domains, there is a discrete set of possible wavenumbers $k_n = 2n\pi/L$, where L is the domain size and n is an integer. Substituting the perturbed solutions $u^{\pm}(x,t) = u_*^{\pm} + v^{\pm}(x,t)$ into the linearised hyperbolic system leads to the following equations

$$\begin{aligned}
\frac{\partial v^+}{\partial t} + \gamma \frac{\partial v^+}{\partial x} &= -\lambda^+[u_*^+, u_*^-]v^+ + \lambda^-[u_*^+, u_*^-]v^- \\
&\quad - u_*^+ \lambda_u^+ (K * v^+) + u_*^- \lambda_u^- (K * v^-), \\
\frac{\partial v^-}{\partial t} - \gamma \frac{\partial v^-}{\partial x} &= \lambda^+[u_*^+, u_*^-]v^+ - \lambda^-[u_*^+, u_*^-]v^- \\
&\quad + u_*^+ \lambda_u^+ (K * v^+) - u_*^- \lambda_u^- (K * v^-).
\end{aligned}$$

Here, $\lambda_u^{\pm}$ are the derivatives of $\lambda^{\pm}$ with respect to $u = (u^+, u^-)$, which appear in the Taylor expansion of $\lambda^{\pm}$ about the steady states (u_*^+, u_*^-). Re-writing these equations in terms of $a_{\pm} e^{\sigma t + ikx}$, we obtain (after simplifying the exponentials $e^{\sigma t + ikx}$)

$$\begin{aligned}
&a_+\big(\sigma + \gamma ik + \lambda^+[u_*^+, u_*^-] + u_*^+ \lambda_u^+ \hat{K}(k)\big) \\
&\quad + a_-\big(-\lambda^-[u_*^+, u_*^-] - u_*^- \lambda_u^- \hat{K}(k)\big) = 0, \\
&a_+\big(-\lambda^+[u_*^+, u_*^-] - u_*^+ \lambda_u^+ \hat{K}(k)\big) \\
&\quad + a_-\big(\sigma - \gamma ik + \lambda^-[u_*^+, u_*^-] + u_*^- \lambda_u^- \hat{K}(k)\big) = 0,
\end{aligned}$$

where $\hat{K}(k)$ is the Fourier transform of the interaction kernel $K(s)$:

$$\hat{K}(k) = \int K(s)e^{iks}ds. \tag{8.7}$$

To find a non-trivial solution for this algebraic system, we impose that the determinant is zero, and obtain the characteristic equation that connects the growth rate σ of the perturbations with the wavenumber k:

$$\sigma^2 + \sigma A(k) + B(k) = 0, \tag{8.8}$$

where $A(k)$ and $B(k)$ are nonlinear terms that depend on the parameters of the system and on the steady states. The expression $\sigma = \sigma(k)$ is called a *dispersion relation*.

If $Re(\sigma(k)) > 0$ for some $k = k_n$, we say that the homogeneous steady state (u_*^+, u_*^-) is unstable to spatial perturbations. Otherwise, if $Re(\sigma(k)) < 0$ for all k, we say that the steady state is linearly stable. Note that since we assumed a finite domain (to be able to compare the analytical stability results with the numerical results, as in [11, 14]), the possible unstable wavenumbers k_n and the corresponding spatial wavelengths of allowable patterns could depend on the boundary conditions. The most unstable wavenumber k_n (i.e., the wavenumber for which $\sigma(k_n)$ has the largest positive value) gives—at least for small time where the linear stability analysis is valid—the number of "peaks" (i.e., aggregations) that form in the domain. In Fig. 8.2 we show a caricature description of (a) a typical example of dispersion relation for which the wavenumber k_2 is unstable, and (b) the corresponding two-peak pattern that emerges (at least for small time). (Compare Fig. 8.2a with Fig. 4.7 which showed a non-standard dispersion relation for a class of local hyperbolic systems introduced in [15].) If the eigenvalues $\sigma(k_n)$ have only real parts then the spatial pattern emerges as a result of real

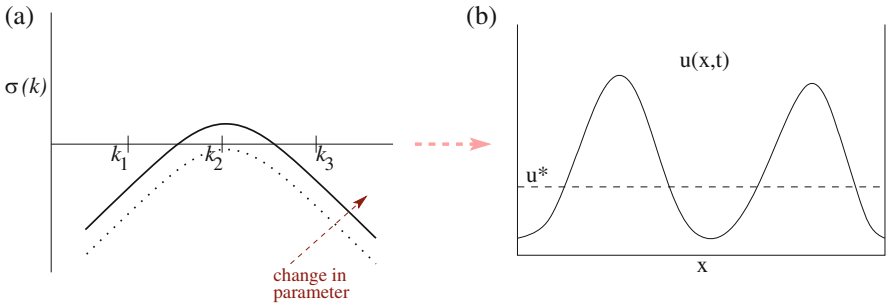

Fig. 8.2 Caricature description of (**a**) a typical example of dispersion relation for which the wavenumber k_2 becomes unstable (as we vary a certain model parameter), and (**b**) the corresponding two-peak pattern $u(x, t)$ that emerges (at least for small time). The dashed line shows the spatially homogeneous solution

(steady state) bifurcations, and the aggregations that form are motionless (e.g., stationary pulses; see also Fig. 1.9a). If, on the other hand, the eigenvalues $\sigma(k_n)$ have complex parts (i.e., $Im(\sigma(k_n)) \neq 0$) then the spatial pattern emerges as a result of complex (Hopf) bifurcations, and the aggregations that form are moving through space (e.g., travelling pulses; see also Fig. 1.9b). We will return to the discussion of real and complex bifurcations in the next section. It is possible that multiple wavenumbers become unstable at the same time; see Fig. 5.10. The spatially heterogeneous solution that emerges, is the sum of the unstable modes: $u(x,t) = \sum_{n1}^{n2} C_n e^{\sigma(k_n)t} cos(k_n x)$. The mode-mode interactions could give rise to more complex spatial and spatio-temporal patterns, as discussed in Chap. 5.

To conclude this brief discussion on linear stability analysis, we emphasise that even if the small perturbations $v^{\pm}$ grow exponentially with time, they are eventually bounded by the nonlinear terms in the reaction-advection equations. If the solution of the PDE is bounded in time, a spatially heterogeneous solution will emerge. For a more detailed discussion of linear stability analysis on pattern formation in partial differential equations in biology (including the stability of steady states for 2D models), we refer the reader to the seminal book by Murray [8].

8.2 Basic Notions of Bifurcation Theory

To be able to understand the changes in the patterns exhibited by various (finite and infinite dimensional) dynamical systems, one needs to have some basic notions of *bifurcation theory*, i.e., the mathematical theory that studies changes in the qualitative or topological structure of a family of differential equations. The term "*bifurcation*" was first introduced by Henri Poincaré in [16]. A bifurcation occurs when a small change in a parameter value (i.e., the bifurcation parameter) leads to a qualitative change in the behaviour of a system. Since in the mathematical literature there are several very good textbooks on bifurcation theory [3, 6, 7, 17, 18], the aim of this chapter is not to give a detailed exposition of the topic, but rather to give the reader enough information to follow the discussion in the previous chapters regarding the mechanisms behind the formation of various patterns. In the following, we will assume that the reader has basic notions of dynamical systems (both finite dimensional and infinite dimensional) and functional analysis; see also the books by Strogatz [7], Robinson [19] and Evans [20].

Even if this monograph focuses on PDEs, we decided to start this brief review of basic notions of bifurcation theory by focusing first on classical bifurcations for ODEs (one dimensional and two dimensional). Our reason for this choice is based on (1) the importance of these classical bifurcations for understanding the long-term dynamics of spatially homogeneous populations (i.e., populations with individuals evenly distributed over the domain), and (2) the importance of these bifurcations in the reduction of infinite-dimensional (PDE) systems to finite-dimensional systems (via Central Manifold reduction, Lyapunov-Schmidt reduction, or weakly nonlinear analysis). In regard to point (1), we note that the class of 1D nonlocal hyperbolic

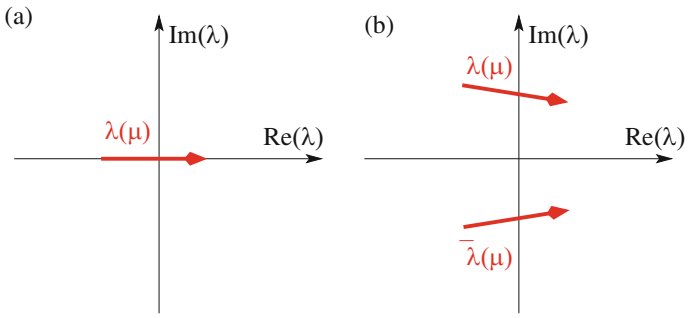

Fig. 8.3 Caricature description of the eigenvalues that generate real and complex bifurcations, as we vary a generic parameter μ. (**a**) Real eigenvalues $\lambda(\mu)$; (**b**) Complex eigenvalues ($\lambda(\mu)$ and $\overline{\lambda}(\mu)$). In general, the complex eigenvalues cross the imaginary axis with nonzero slopes

models introduced in [11] was shown to display spatially homogeneous solutions $(u^+, u^-) = (u_*^+, u_*^-)$ with $u_*^+ \neq u_*^-$ (corresponding to more individuals facing one direction than the other direction), and these solutions arise via saddle-node and (subcritical) pitchfork bifurcations [11, 14]; see also Fig. 8.1. In regard to point (2), we will see in Sect. 8.5 that we could understand the dynamics of a nonlocal hyperbolic system near a bifurcation point via the dynamics of an ODE for the amplitude of the perturbations as given by Eq. (8.38).

The *codimension ("codim") of a bifurcation* is given by the number of parameters that need to be varied to reach the locus of the bifurcation. Throughout Chap. 5 we referred to *codimension-1 bifurcations* (where one parameter μ was varied) and *codimension-2 bifurcations* (where two parameters, μ_1 and μ_2, were varied at the same time). In the following we will review briefly four codimension-1 classical bifurcations from fixed points: saddle-node bifurcations, transcritical bifurcations, pitchfork bifurcations and Hopf bifurcations. The first three types of bifurcations are stationary (or steady state), i.e., they correspond to a real eigenvalue $\lambda(\mu)$ passing through zero (see Fig. 8.3a). The fourth bifurcation is oscillatory, with the real part of the complex eigenvalues passing through zero, while the imaginary part is nonzero (see Fig. 8.3b). Since the majority of bifurcations identified in the literature of hyperbolic and kinetic models for self-organised behaviours are local, here we focus mainly on these local bifurcations. However, towards the end of this section we will also mention briefly some examples of nonlocal bifurcations (e.g., homoclinic loops) exhibited by the nonlocal hyperbolic models (5.14).

The structure of the bifurcations is encoded in their normal forms (i.e., simplified equations that determine the dynamics of the system/bifurcation), and all systems that exhibit a bifurcation are locally topologically equivalent to the normal form of the bifurcation. Thus, in the following we describe briefly the normal forms corresponding to four classical codimension-1 local bifurcations. To this end we

start with the following differential equation in $\mathbb{R}$:

$$\frac{du}{dt} = f(u, \mu), \tag{8.9}$$

where u is a real-valued function of time t ($u \in \mathbb{R}^+$) and μ is a real bifurcation parameter ($\mu \in \mathbb{R}$). Assume that the vector field $f(u, \mu)$ satisfies the following two conditions:

$$f(0, 0) = 0, \quad \frac{\partial f(0, 0)}{\partial u} = 0. \tag{8.10}$$

The first condition says that $u = 0$ is an equilibrium point when $\mu = 0$, while the second condition is necessary for the appearance of a local bifurcation at $\mu = 0$. (If $\partial f(0, 0)/\partial u \neq 0$, the implicit function theorem says that $f(u, \mu) = 0$ has a unique solution $u = u(\mu)$ in the neighbourhood of 0, and thus $u = 0$ is the only solution for $\mu = 0$ or sufficiently small μ, leading to the impossibility of having a bifurcation for small values of μ [5]).

- **Saddle-node bifurcations.** Assume that in addition to conditions (8.10), the vector field $f(u, \mu)$ satisfies also two other conditions:

$$\frac{\partial f}{\partial \mu}(0, 0) = 1 \neq 0, \quad \frac{\partial^2 f}{\partial u^2}(0, 0) = c \neq 0. \tag{8.11}$$

  Following a Taylor expansion of $f(u, \mu)$ near $(0, 0)$, we obtain the following truncated equation

$$\frac{du}{dt} = \mu + cu^2. \tag{8.12}$$

  This normal form Eq. (8.12) approximates the dynamics of the full model (8.9). Equation (8.12) has the following fixed points: $u = 0$ for $\mu = 0$, and $u = \pm\sqrt{-\mu/c}$ for $\mu/c < 0$. The stability of the fixed points is determined by the sign of derivative $\frac{\partial f}{\partial u}$. For $c > 0$ the non-trivial fixed points exist only when $\mu < 0$, and $+2c\sqrt{-\mu/c}$ is unstable while $-2c\sqrt{-\mu/c}$ is stable (see Fig. 8.4a). For $c < 0$ the non-trivial fixed points exist only when $\mu > 0$, and $+2c\sqrt{-\mu/c}$ is stable while $-2c\sqrt{-\mu/c}$ is unstable (see Fig. 8.4a).
- **Transcritical bifurcations.** Assume that in addition to conditions (8.10), the vector field $f(u, \mu)$ satisfies also three other conditions:

$$\frac{\partial f}{\partial \mu}(0, 0) = 0, \quad \frac{\partial^2 f}{\partial u \partial \mu}(0, 0) = 1 \neq 0, \quad \frac{\partial^2 f}{\partial u^2}(0, 0) = 2c \neq 0. \tag{8.13}$$

  Expanding $f(u, \mu)$ in Taylor series about $(0, 0)$, and incorporating the above conditions leads to the following truncated normal form equation for a transcritical

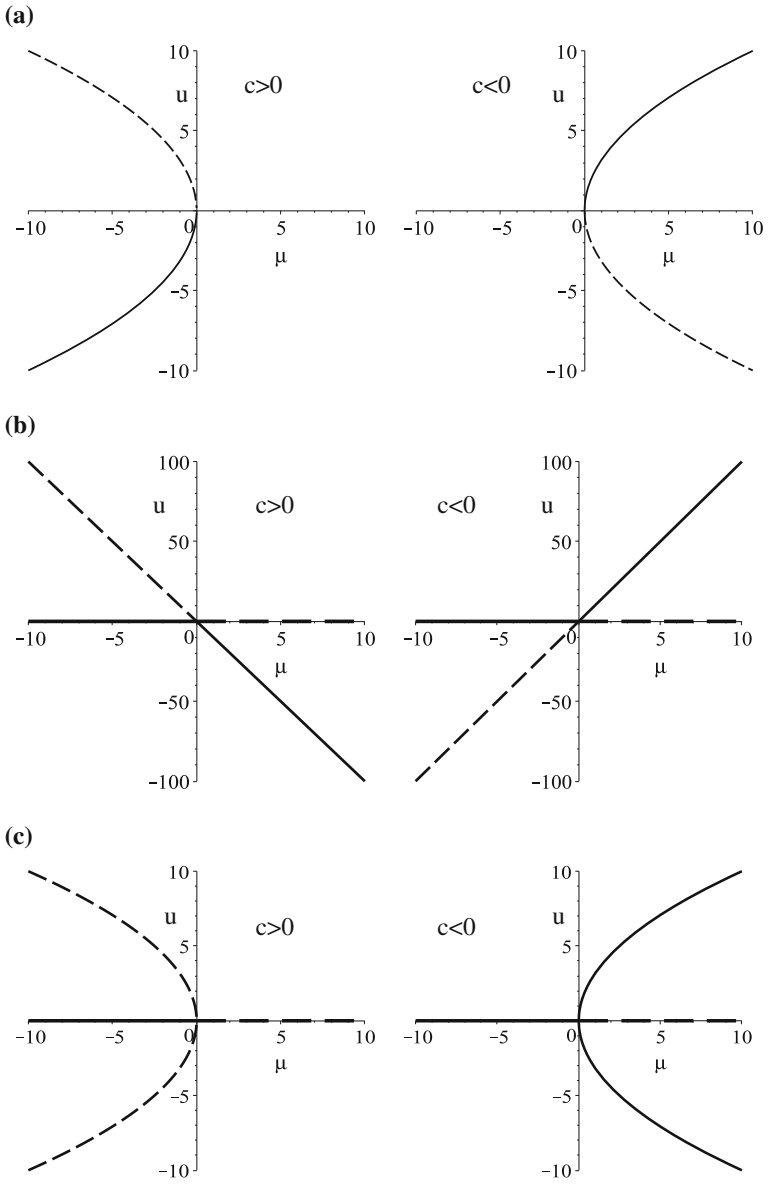

Fig. 8.4 Bifurcation diagrams in the (μ, u) plane of the normal form equations corresponding to: (**a**) Saddle-node bifurcations; (**b**) Transcritical bifurcations; (**c**) Pitchfork bifurcations. The solid continuous curves describe stable states, while the dashed curves describe unstable states

bifurcation:

$$\frac{du}{dt} = \mu u + cu^2, \quad u, \mu, c \in \mathbb{R}. \tag{8.14}$$

The fixed points of this equation are $u = 0$ and $u = -\mu/c$. Simple linear stability analysis shows that $u = 0$ is stable for $\mu < 0$ and unstable for $\mu > 0$, while $u = -\mu/c$ is stable for $\mu > 0$ and unstable for $\mu < 0$ (see Fig. 8.4b).

- **Pitchfork bifurcations.** In many cases, the models have some sort of symmetry. The simplest symmetry is the reflection symmetry $u \to -u$. We need to emphasise that this symmetry is not biologically realistic in this form, since one cannot have a population with negative density $-u$. However, in some biological systems one could have a slightly different version of this symmetry: $u \to U - u$, with U a maximum populations size; see the steady states in Fig. 8.1a, which are symmetric with respect to $u = A/2$, where $A = (1/L)\int_0^L [u^+(x) + u^-(x)]dx$ denoted the total population density. Assume now that the vector field $f(u, \mu)$ is odd with respect to u, satisfies conditions (8.10) and also the following conditions:

$$\frac{\partial f}{\partial \mu}(0, 0) = 0, \quad \frac{\partial^2 f}{\partial \mu \partial u}(0, 0) = 1 \neq 0, \quad \frac{\partial^3 f}{\partial u^3}(0, 0) = 6c \neq 0. \tag{8.15}$$

Following a Taylor expansion of $f(u, \mu)$ near $(0, 0)$, we obtain the following truncated normal form equation

$$\frac{du}{dt} = \mu u + cu^3. \tag{8.16}$$

This equation has the following fixed points: $u = 0$ for any μ, and $u = \pm\sqrt{-\mu/c}$ for $\mu/c < 0$. These non-trivial points exist for $\mu > 0$ when $c < 0$ and for $\mu < 0$ when $c > 0$. The trivial point is stable for $\mu < 0$ and unstable for $\mu > 0$. The nontrivial point $\pm\sqrt{-\mu/c}$ is unstable for $c > 0$ and $\mu < 0$, and stable for $c < 0$ and $\mu > 0$ (see Fig. 8.4c). The appearance of stable branches for $\mu > 0$ shown in the right panel of Fig. 8.4c occurs through a supercritical bifurcation, while the appearance of unstable branches for $\mu < 0$ in the left panel of Fig. 8.4c occurs through a subcritical bifurcation.

Remark 8.1 The pitchfork bifurcations that give rise to the spatially-homogeneous steady states graphed in Fig. 8.1a are the result of the symmetries of the nonlocal hyperbolic system (8.6) with the five communication mechanisms described in Table 5.1. For symmetric communication mechanisms (i.e., $p_+ = p_- = 1.0$), the bifurcations shown in Fig. 8.1a are perfect. However, as we perturb the perception mechanisms (i.e. $p_+ = 1.05$, $p_- = 0.95$), thus assuming asymmetric communication, we obtain imperfect bifurcation diagrams as a result of symmetry breaking, as shown in Fig. 8.1b.

Remark 8.2 The three bifurcations of fixed points discussed above in the one-dimensional case (i.e., saddle-node, transcritical and pitchfork bifurcations) can be easily generalised to two and higher dimensions. For example, for the normal form equations in 2D (with variables u and v) we can assume that the dynamics in the u-direction is given by the normal forms discussed above, and the dynamics in the v-direction is exponentially damped [7]:

$$\begin{aligned}
&\frac{du}{dt} = \mu + cu^2, \quad \frac{dv}{dt} = -v,\\
&\frac{du}{dt} = \mu u + cu^2, \quad \frac{dv}{dt} = -v,\\
&\frac{du}{dt} = \mu u + cu^3, \quad \frac{dv}{dt} = -v.
\end{aligned}$$

For a more detailed discussion regarding the generalisation of these bifurcations to higher dimensions, and the fact that the addition of higher dimensions does not influence the bifurcations (which still occur along a one-dimensional space), see [7].

- **Hopf bifurcations.** Consider now the following differential equation in $\mathbb{R}^2$:

$$\frac{d\mathbf{u}}{dt} = \mathbf{f}(\mathbf{u}, \mu), \quad \text{with } \mathbf{u} = (u, v) \in \mathbb{R}^2, \ \mu \in \mathbb{R}. \tag{8.17}$$

Assume that the vector field $\mathbf{f} \in \mathbb{R}^2$ satisfies $\mathbf{f}(\mathbf{0}, 0) = 0$ (i.e., $\mathbf{u} = \mathbf{0}$ at $\mu = 0$). The presence of a bifurcation is determined by the linearisation of $\mathbf{f}(\mathbf{u}, \mu)$ at $(\mathbf{0}, 0)$, as given by the Jacobian matrix $J = D_{\mathbf{u}}\mathbf{f}(\mathbf{0}, 0)$. Moreover, assume that the Jacobian matrix has the following canonical form

$$J = \begin{pmatrix} \alpha(\mu) & \beta(\mu) \\ -\beta(\mu) & \alpha(\mu) \end{pmatrix}, \tag{8.18}$$

and at $\mu = 0$ we have $\alpha(0) = 0$, $\alpha'(0) \neq 0$ and $\beta(0) = \omega \neq 0$ (so that in the neighbourhood of $\mu = 0$, we have $det(J) \neq 0$). The linearised equations (8.17) are

$$\frac{du}{dt} = \alpha(\mu)u + \beta(\mu)u + O(u^2, v^2, uv), \tag{8.19a}$$

$$\frac{dv}{dt} = -\beta(\mu)u + \alpha(\mu)v + O(u^2, v^2, uv). \tag{8.19b}$$

Let us introduce a new variable $z = u + iv$, which allows us to re-write Eq. (8.19) as

$$\frac{dz}{dt} = \big(\alpha(\mu) - i\beta(\mu)\big)z + O(|z|^2), \quad \text{as } |z| \to 0. \tag{8.20}$$

Making a transformation of the form $\psi = z + S(z, \bar{z}, \mu)$, with $S \approx O(|z|^2)$ leads to a normal form equation

$$\frac{d\psi}{dt} = \big(\alpha(\mu) - i\beta(\mu)\big)\psi + A(\mu)|\psi|^2\psi + O(|\psi|^4), \tag{8.21}$$

with $A(\mu) = a(\mu) + ib(\mu)$ a complex term.

To understand the dynamics of this normal form equation, it is better to introduce the polar coordinates $\psi = re^{i\theta}$ (with $r > 0$ and $0 \leq \theta \leq 2\pi$), which transforms Eq. (8.21) into the following system:

$$\frac{dr}{dt} = \alpha(\mu)r + a(\mu)r^3, \tag{8.22a}$$

$$\frac{d\theta}{dt} = -\beta(\mu) + b(\mu)r^2. \tag{8.22b}$$

Note that Eq. (8.22a) is the normal form for a pitchfork bifurcation in r. This suggests that a Hopf bifurcation is a pitchfork bifurcation in r direction, with a rotation in θ direction. From the phase equation (8.22b) we obtain $\theta = \theta_0 + \omega(\mu)t$, with $\omega(\mu) = -\beta(\mu) - b(\mu)\alpha(\mu)/a(\mu) \to -\beta(0)$ as $\mu \to 0$ (since we assumed above that $\alpha(0) = 0$).

The fixed points of the amplitude equation (8.22a) are $r = 0$ and $r = \sqrt{-\alpha(\mu)/a(\mu)}$. We assume that $a(\mu) \neq 0$ in the neighbourhood of $\mu = 0$. This non-trivial solution branch corresponds to a periodic solution with period $2\pi/|\omega(\mu)| \to 2\pi/|\omega(0)|$ as $\mu \to 0$. The stability of these two solutions depends on the signs of $\alpha(\mu)$ and $a(\mu)$. While we keep these two functions general enough to not discuss their signs, we graph in Fig. 8.5 the two possible Hopf bifurcations: (a) a supercritical bifurcation, and (b) a subcritical bifurcation.

The Hopf bifurcation represents one way through which limit cycles are created or destroyed. However, limit cycles can be destroyed when two different cycles (a

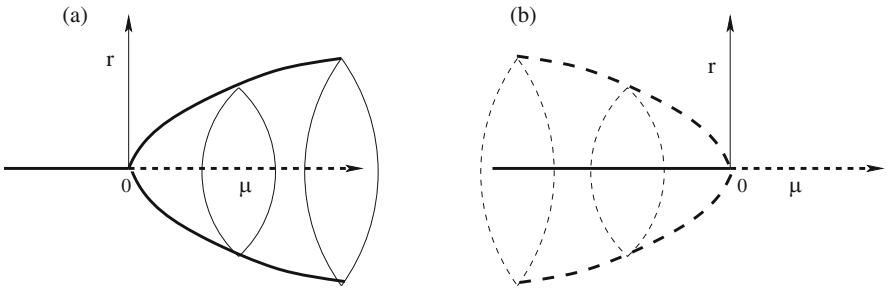

Fig. 8.5 Bifurcation diagram for: (**a**) a supercritical Hopf bifurcation; (**b**) a subcritical Hopf bifurcation. Continuous solid curves indicate stable branches, while dashed curves indicate unstable branches

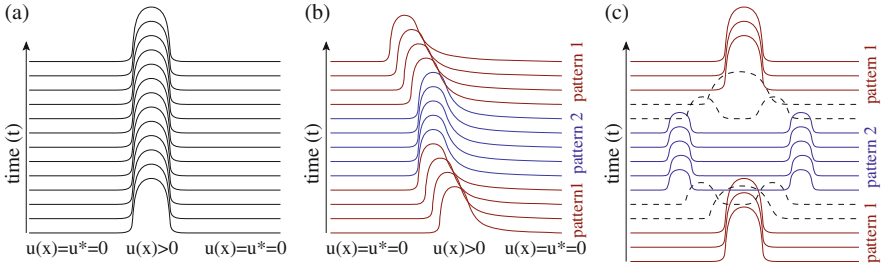

Fig. 8.6 Caricature description of (**a**) a homoclinic orbit (in the form of a stationary pulse connecting two zero steady states); (**b**) a heteroclinic cycle connecting a travelling pulse (pattern 1—in red) and a stationary pulse (pattern 2—in blue); (**c**) a heteroclinic cycle connecting two stationary states (pattern 1—in red; and pattern 2—in blue)

stable and an unstable cycle) coalesce via a *saddle-node bifurcation of cycles* [7]. This is a *global bifurcation* since it does not occur anymore near a fixed point. Note that global bifurcations occur when larger invariant sets, such as periodic orbits, collide with each other or with other equilibria. In the following we discuss briefly two types of global bifurcations that have been shown to be exhibited by the nonlocal hyperbolic systems (8.7).

- **Homoclinic bifurcations** occur when a limit cycle moves closer to a saddle point until it coalesces with it becoming a homoclinic loop. In the context of partial differential equations, a homoclinic loop describes a travelling pulse or a stationary pulse, i.e., a nonzero solution $u(z) = u(x - ct)$ which connects (as $z \to \pm\infty$) the stable and unstable manifolds of a spatially homogeneous steady state (usually $u^* = 0$; see Fig. 5.7a, b) and propagates with speed $c > 0$ (for travelling pulses) or $c = 0$ (for stationary pulses). See Fig. 8.6a for a caricature description of a homoclinic loop.
- **Heteroclinic bifurcations** occur when a cycle connects different unstable (spatially homogeneous or heterogeneous) states, via their stable and unstable manifolds. These bifurcations are more difficult to be identified for the hyperbolic and kinetic models discussed in the previous chapters, due to the large parameter space that needs to be investigated. The nonlocal hyperbolic models (8.7) can exhibit heteroclinic cycles that connect two stationary states (R. Eftimie—unpublished results), which are the result of Steady-state/Steady-state heteroclinic bifurcations; see Fig. 8.6c for a caricature description of a heteroclinic cycle connecting two different stationary states. Figure 8.6b shows a caricature description of a heteroclinic cycle connecting a stationary state and a travelling pulse (which is somehow similar—at macroscopic level—to the semi-zigzag dynamics shown in Fig. 5.7f, but for one aggregation peak). We need to emphasise here that the analytical study of heteroclinic bifurcations in hyperbolic and kinetic models is still an open problem at this moment.

Remark 8.3 As emphasised by Knobloch and Aulbach [21], the various bifurcating objects (which are formed of small bounded solutions, such as steady states or orbits) always lie on centre manifolds. Therefore, from a bifurcation point of view, it is enough to study the flow of a system on the centre manifold. We will return to the existence of these centre manifolds (for both ODEs and PDEs) in Sect. 8.6.

8.3 Symmetry of Hyperbolic and Kinetic Equations

Symmetry and symmetry breaking phenomena are very common in self-organised biological communities, as shown by various experiments [22–26]. From a mathematical point of view, many of the models for self-organised patterns in biological aggregations that we discussed in the previous chapters have some sort of symmetry (either as a result of the equations themselves, or as a result of the domain and the boundary conditions—e.g., periodic conditions). The presence of symmetries is welcomed since it allows us to reduce the size of the system (which reduces the cost of solving the equations). However, very few studies on kinetic and hyperbolic models for biological aggregations recognised the importance of these symmetries on cell/bacterial/animal pattern formation [27–30]. Since the symmetries of systems of differential equations (ODEs and PDEs) are usually discussed in terms of a group of transformations of variables that preserve the structure of the equations and their solutions, in the following we give a brief introduction to the most common notions of group theory that are used to understand the symmetries of a model. To this end, we follow the approaches in [2, 3].

Definition 8.3 A *group* Γ is a set $\{\gamma_1, \gamma_2, \gamma_3, \ldots\}$ together with an operation "$\cdot$" (which maps $\Gamma \times \Gamma \to \Gamma$) that satisfies the group axioms:

- The group is closed under the group operation: for any $\gamma_1, \gamma_2 \in \Gamma$, then $\gamma_3 = \gamma_1 \cdot \gamma_2 \in \Gamma$;
- Associativity axiom: for any $\gamma_1, \gamma_2, \gamma_3 \in \Gamma$, then $(\gamma_1 \cdot \gamma_2) \cdot \gamma_3 = \gamma_1 \cdot (\gamma_2 \cdot \gamma_3)$;
- Identity axiom: there exists an element $e \in \Gamma$ such that $\gamma \cdot e = e \cdot \gamma = \gamma$, for any $\gamma \in \Gamma$;
- Inverse axiom: for any $\gamma \in \Gamma$, there exists an element $\gamma^{-1} \in \Gamma$ such that $\gamma \cdot \gamma^{-1} = \gamma^{-1} \cdot \gamma = e$.

Let us now summarise some of the most common groups that are important in pattern formation [3]:

- **Lie** group: a finite-dimensional smooth manifold together with a group structure, such that the group operations are smooth maps;
- $\mathbf{D}_n$: the dihedral group of order $2n$, generated by rotations and reflections in the plane that preserve a regular polygon with n sides. For example, $\mathbf{D}_2$ is the symmetry group of a rectangle, and is isomorphic with the direct product $\mathbf{Z}_2 \times \mathbf{Z}_2$;
- $\mathbf{Z}_n$: the cyclic group of order n, generated only by rotations;

- $\mathbf{S}^1$: the circle group of unit complex numbers. The group characterises the periodic solutions;
- $\mathbf{O}(n)$: the orthogonal group in $\mathbb{R}^n$, which consists of $n \times n$ orthogonal matrices (i.e., real matrices A with the property that their transposes are equal to their inverses: $A^\top = A^{-1}$). The group is isomorphic to the group of all rotations and reflections in $\mathbb{R}^n$ that keep the origin fixed;
- $\mathbf{SO}(n)$: the special orthogonal group consisting of $n \times n$ orthogonal matrices with determinant 1. It is a subgroup of $\mathbf{O}(n)$, and is sometimes called the *rotation group*, since in $\mathbb{R}^2$ and $\mathbb{R}^3$ its elements are the rotations around a point ($n = 2$) and around a line ($n = 3$);
- $\mathbf{SO}(2)$: the special orthogonal group in $\mathbb{R}^2$, which consists of rotations

$$R_\theta = \begin{pmatrix} \cos(\theta) & -\sin(\theta) \\ \sin(\theta) & \cos(\theta) \end{pmatrix} \tag{8.23}$$

  in the plane. This group is isomorphic with $\mathbf{S}^1$, since if we write a complex number $e^{i\theta} = \cos(\theta) + i\sin(\theta)$ as a 2×2 real matrix

$$e^{i\theta} \leftrightarrow \begin{pmatrix} \cos(\theta) & -\sin(\theta) \\ \sin(\theta) & \cos(\theta) \end{pmatrix}, \tag{8.24}$$

  then the unit complex number corresponds to the 2×2 orthogonal matrix with unit determinant.
- $\mathbf{T}^n = \mathbf{S}^1 \times \ldots \times \mathbf{S}^1$: the n-torus;
- $\mathbf{E}(2)$: the Euclidean group of the plane, generated by rotations, reflections and translations.

To describe how the elements of a group act on some space in a way that preserves the structure of that space, we introduce the notion of *group action* [3]:

Definition 8.4 Consider Γ a Lie group and V a vector space. The *action* of Γ on V is a homomorphism $\rho : \Gamma \to GL(V)$ (with $GL(V)$ the general linear group of invertible matrices on V). We denote the group action $\rho(\gamma)(v) = \gamma \cdot v$.

Definition 8.5 A dynamical system that has an appropriate symmetry is called an *equivariant dynamical system*. In this case, the bifurcation theory is called *equivariant bifurcation theory*.

Consider the following generic dynamical system that depends on a parameter $\mu \in \mathbb{R}$:

$$\frac{du}{dt} = f(u, \mu), \quad \text{with } u \in \mathbb{R}^n, \ f : \mathbb{R}^n \times \mathbb{R} \to \mathbb{R}^n. \tag{8.25}$$

Definition 8.6 We say that system (8.25) is *equivariant* with respect to a group Γ if $f(\gamma \cdot u, c) = \gamma \cdot f(u, c)$, for all $\gamma \in \Gamma$. Here "$\cdot$" denotes the group action; see [17].

Note that a group element $\gamma \in \Gamma$ is a symmetry of system (8.25) if given a solution $u(t)$, then $\gamma \cdot u(t)$ is also a solution of (8.25). We define the *group orbit* of a solution u as $\Gamma u = \{\gamma \cdot u, \text{ for } \gamma \in \Gamma\}$ (i.e., the group orbit is the set of solutions connected by the group action). Therefore, if one knows a solution of a differential equation, the whole group orbit of this solution will be solutions, too.

One can classify the solutions with respect to their symmetry groups by computing the isotropy subgroups [3, 27]:

Definition 8.7 Consider the action "$\cdot$" of a group Γ on a vector space V. The *isotropy subgroup* of a point $v \in V$ is defined as

$$\Sigma_v := \{\gamma \in \Gamma | \gamma \cdot v = v\}. \tag{8.26}$$

In other words, the isotropy subgroup of v is the set of all elements (symmetries) that leaves v invariant.

Let us focus now on the notion of *conjugacy*:

Definition 8.8 We say that two group elements $a_1, a_2 \in \Gamma$ are *conjugate* (or in the same conjugacy class) if there exist a group element $\gamma \in \Gamma$ such that $a_1 = \gamma \cdot a_2 \cdot \gamma^{-1}$.

One can further show that solutions u and $\gamma \cdot u$ of (8.25) have *conjugate isotropy subgroups*: $\Sigma_{\gamma \cdot u} = \gamma \cdot \Sigma_u \cdot \gamma^{-1}$. This result is important since it allows us to classify solutions in terms of the conjugacy classes of their isotropy subgroups. More precisely, the isotropy subgroups of all points on an orbit of the action of a group Γ belong to the same conjugacy class. Because the points on the same group orbit have similar existence and stability characteristics, we usually assume (in a loose sense) that the isotropy subgroups are similar [2]. When classifying the solutions of a system of differential equations, we can simplify our analysis by ignoring those solutions corresponding to similar isotropy subgroups (see for example [27] for the classification of steady states solutions for the amplitude equations that resulted from a weakly nonlinear analysis of a Hopf/Hopf bifurcation with $\mathbf{O}(2)$ symmetry).

For the dynamical system (8.25), to find an equilibrium solution u with isotropy subgroup Σ_u, we can restrict our search to the fixed point subspace of this isotropy subgroup [27]:

Definition 8.9 Consider an isotropy subgroup $\Sigma_v \in \Gamma$. The *fixed point subspace* of Σ_v is defined as

$$Fix(\Sigma_v) := \{v \in V | \sigma \cdot v = v, \text{ for all } \sigma \in \Sigma\}. \tag{8.27}$$

We conclude this list of definitions necessary for understanding the symmetries of differential equations, by discussing subspaces that are invariant under the action of a group Γ (since these are the spaces that support bifurcations) [3]:

Definition 8.10 Consider a subspace $V \in \mathbb{R}^n$. We say that V is Γ*-invariant* if $\gamma \cdot V = V$ for any $\gamma \in V$.

Definition 8.11 If the subspace $V \in \mathbb{R}^n$ is such that it has only two Γ invariant subspaces, namely V and $\{0\}$, we say that V is Γ*-irreducible*. We say that the action of Γ is *absolutely irreducible* if the only linear maps that commute with the action of Γ on V are the scalar multiples of the identity: $\{aI, a \in \mathbb{R}\}$.

The above notion of absolute irreducibility is important to the Equivariant Branching Lemma, which predicts the existence of branches of symmetry-breaking solutions near bifurcations:

Theorem 8.1 (Equivariant Branching Lemma [3]) *Consider $\Gamma \subset \mathbf{O}(n)$ a compact Lie group acting absolutely irreducible on $\mathbb{R}^n$. Consider the Γ-equivariant bifurcation problem*

$$\frac{du}{dt} = f(u, \mu), \tag{8.28}$$

with $f : \mathbb{R}^n \times \mathbb{R} \to \mathbb{R}^n$ satisfying the following conditions: $f(0, \mu) = 0$, $D_u f(0, \mu) = c(\mu)I$ (where I=identity operator), with $c(0) = 0$ (bifurcation condition) and $c'(0) \neq 0$ (eigenvalue crossing condition). If Σ is an isotropy subgroup of Γ with $\dim Fix(\Sigma) = 1$, then there exist a unique smooth branch of solutions to $f(u, \mu) = 0$, with symmetry given by the isotropy group Σ.

Note that, depending on some conditions for the bifurcation equation $f(u, \mu) = 0$ in $Fix(\Sigma)$, and on whether $\Sigma = \Gamma$ or $\Sigma < \Gamma$, one can distinguish between saddle-node bifurcation, transcritical bifurcation or pitchfork bifurcation (see Theorem 2.3.2 in [4]).

The solution branches that bifurcate from the fixed point $u = 0$ are called *primary branches* (see Fig. 5.11b, c). It is possible to have other solutions that bifurcate from these primary branches (further away from the original fixed point), and they give rise to *secondary branches* (see Fig. 5.11b, c). These secondary branches can lead to an exchange in the stability of solutions.

Returning now to the nonlocal hyperbolic and kinetic equations discussed in Chaps. 4–6, we note that the majority of those models exhibit $\mathbf{O}(2)$ or $\mathbf{SO}(2)$ symmetries:

- translations: $T_\theta \cdot u(x, t) = u(x - \theta, t)$, with $\theta \in [0, L)$;
- reflections (with respect to the domain boundary): $\kappa \cdot (u^+(x, t), u^-(x, t)) = \big(u^-(L - x, t), u^+(L - x, t)\big)$;

Since the boundary conditions used for the majority of 1D nonlocal hyperbolic and kinetic models discussed in this study [11, 14, 27, 28] are periodic, the translation operator T_θ (= rotation operator on a 1D line) generates a group isomorphic to $\mathbf{SO}(2)$. Moreover, one can check that $T_\theta \circ \kappa = \kappa \circ T_\theta^{-1}$, and thus the translation and reflection operators generate a group isomorphic to $\mathbf{O}(2)$ [30]. It was also shown in various studies [27–30] that the 1D nonlocal hyperbolic system (5.14)

with communication mechanisms M1–M5 (see also Fig. 5.5 and Table 5.1) is $\mathbf{O}(2)$-invariant: if $u(x,t) = (u^+(x,t), u^-(x,t))$ is a solution of (5.14), then $T_\theta \cdot u(x,t)$ and $\kappa \cdot u(x,t)$ are also solutions of (5.14).

The symmetry structure of nonlocal 1D hyperbolic models (5.14), together with the types of bifurcations exhibited by these models (i.e., real or complex bifurcations), was used in [27, 28] to classify rigorously the patterns emerging near codimension-2 Hopf/Hopf and Hopf/Steady-state bifurcations, via the isotropy subgroups generated by the $\mathbf{O}(2)$ action on the elements of the hyperbolic system. As an example, we show in Table 8.1 the isotropy subgroups of the $\mathbf{O}(2) \times \mathbb{T}^2$ action, together with the corresponding types of solutions. For more details, we refer the reader to the studies by Buono and Eftimie [27, 28].

Regarding the 2D kinetic models discussed in this study, we note that there are different studies in the literature which investigate the symmetry and invariance properties of various Vlasov-type and Boltzmann-type equations (mainly in 2D, but a few also in 1D) [31–37]. Some of these studies have shown that the collision integral operator for the Boltzmann equation is $\mathbf{SO}(2)$-invariant [31]. Although none of these studies focused on the application of Boltzmann-like equations to describe the collective movement of cells/bacteria/animals, we expect that many of the models discussed in Chap. 6 are also $\mathbf{SO}(2)$-invariant. Finally, since in Chap. 6 we mentioned the Fokker-Planck equations that were derived from Boltzmann-type models via grazing collision limits, it is worth noting that over the last three decades various mathematical studies in the literature have investigated the symmetries of such Fokker-Planck equations [38–41]. A few studies also focused on the bifurcations around homogeneous and heterogeneous states in Vlasov and Vlasov-Fokker-Plank systems used to describe different physics problems [42]. However, it is expected that biological applications of such systems (see some of the biologically-inspired kinetic models described in Chap. 6) could lead to more complex bifurcations.

8.4 Compact Operators and the Fredholm Alternative

Since the Lyapunov-Schmidt reduction (not discussed in this monograph, but reviewed in [30]) and the weakly-nonlinear analysis (discussed in Sect. 8.5) approaches used to reduce the infinite-dimensional nonlinear PDE systems to finite-dimensional ODE systems to study bifurcation dynamics, are based on Fredholm operators and the Fredholm alternative, in the following we present a few definitions related to these two topics. Consider thus two Banach spaces, X and Y (see also Table 2.1).

Definition 8.12 A *linear operator* (or a *linear transformation*) $T : X \to Y$ is *bounded* if there is a constant M such that

$$||Tu||_Y \leq M||u||_X, \quad \text{for all } u \in X.$$

Table 8.1 Summary of patterns emerging near a Hopf/Hopf bifurcation ($k_3 : k_4$), and the isotropy subgroups for the $\mathbf{O}(2) \times \mathbb{T}^2$ action, as given in [27]

Isotropy subgroups	Solutions	Eigenfunctions
$\Sigma_0 = \mathbf{O}(2) \times \mathbb{T}^2$ (full group)	Spatially homogen.	0
$\Sigma_1 = S(0,0,1) \times S(1,3,0)$	Rotating (travelling) waves	$\alpha_1(T)\mathbf{v_1}e^{i\omega_1 t + ik_3 x}$
$\Sigma_2 = S(0,1,0) \times S(1,0,4)$	Rotating (travelling) waves	$\beta_2(T)\mathbf{w_2}e^{i\omega_2 t + ik_4 x}$
$\Sigma_3 = S(0,0,1) \times \mathbb{Z}_2(\kappa) \times \mathbb{Z}(\frac{L}{6}, \frac{L}{2}, 0)$	Standing waves (ripples)	$\alpha_1(T)(\mathbf{v_1}e^{i\omega_1 t + ik_3 x} + \mathbf{v_2}e^{i\omega_1 t - ik_3 x})$
$\Sigma_4 = S(0,1,0) \times \mathbb{Z}_2(\kappa) \times \mathbb{Z}(\frac{L}{8}, 0, \frac{L}{2})$	Standing waves (ripples)	$\beta_1(T)(\mathbf{w_1}e^{i\omega_2 t + ik_4 x} + \mathbf{w_2}e^{i\omega_2 t - ik_4 x})$
$\Sigma_5 = S(0,0,1) \times \mathbb{Z}(\frac{L}{6}, \frac{L}{2}, 0)$	Modulated standing waves	$\alpha_1(T)\mathbf{v_1}e^{i\omega_1 t + ik_3 x} + \alpha_2(T)\mathbf{v_2}e^{i\omega_1 t - ik_3 x}$
$\Sigma_6 = S(0,1,0) \times \mathbb{Z}(\frac{L}{8}, 0, \frac{L}{2})$	Modulated standing waves	$\beta_1(T)\mathbf{w_1}e^{i\omega_2 t + ik_4 x} + \beta_2(T)\mathbf{w_2}e^{i\omega_2 t - ik_4 x}$
$\Sigma_7 = S(1,3,4)$	Modulated rotating waves	$\alpha_2(T)\mathbf{v_2}e^{i\omega_1 t - ik_3 x} + \beta_2(T)\mathbf{w_2}e^{i\omega_2 t - ik_4 x}$
$\Sigma_8 = S(1,3,-4)$	Modulated rotating waves	$\alpha_2(T)\mathbf{v_2}e^{i\omega_1 t - ik_3 x} + \beta_1(T)\mathbf{w_1}e^{i\omega_2 t + ik_4 x}$
$\Sigma_9 = \mathbb{Z}_2 \times \mathbb{Z}(\frac{L}{2}, \frac{3L}{2}, \frac{4L}{2})$	Modulated rotating waves	$\alpha_1(T)(\mathbf{v_1}e^{i\omega_1 t + ik_3 x} + \mathbf{v_2}e^{i\omega_2 t - ik_3 x}) + \beta_1(T)(\mathbf{w_1}e^{i\omega_2 t + ik_4 x} + \mathbf{w_2}e^{i\omega_2 t - ik_4 x})$
$\Sigma_{10} = \mathbb{Z}_\kappa(0,0,\frac{L}{2}) \times \mathbb{Z}(\frac{L}{2}, \frac{3L}{2}, \frac{4L}{2})$	Modulated rotating waves	$\alpha_1(T)(\mathbf{v_1}e^{i\omega_1 t + ik_3 x} + \mathbf{v_2}e^{i\omega_2 t - ik_3 x}) + \beta_1(T)(\mathbf{w_1}e^{i\omega_2 t + ik_4 x} - \mathbf{w_2}e^{i\omega_2 t - ik_4 x})$

The patterns are defined in the second column, and the approximated solutions (see Eq. (8.46)) are shown in the third column. L describes the domain length

Definition 8.13 A *bounded linear operator* $T : X \to Y$ is *compact* if for each bounded sequence $u_i \subset X$, there exists a subsequence $\{u_{i_k}\}$ such that $\{Tu_{ik}\}$ is convergent.

If $T : X \to Y$ is a bounded linear operator, we define its range ($Ran(T)$) by

$$Ran(T) := \{y \in Y | \exists\, x \in X, \;\; s.t. \;\; Tx = y\},$$

and its kernel ($ker(T)$) by

$$ker(T) = \{x \in X | Tx = 0\}.$$

Definition 8.14 A *Fredholm operator* is a bounded linear operator $T : X \to Y$ with finite-dimensional kernel $ker(T)$ and cokernel $coker(T) = Y/Ran(T)$, and closed range $Ran(T)$. We denote by $\mathscr{F}(X, Y)$ the space of all Fredholm operators between X and Y.

Definition 8.15 The *index* of a Fredholm operator is defined as

$$index(T) = \dim\, ker(T) - \dim\, coker(T)$$

Note that the index of an operator is a measure of how invertible an operator is. In particular, if T is an invertible operator then $index(T) = 0$. The index of a Fredholm operator has some properties:

- If T is a Fredholm operator and K is a compact operator, then $T + K$ is a Fredholm operator and $index(T + K) = index(T)$.
- If T and S are Fredholm operators, the TS is Fredholm and $index(TS) = index(T) + index(S)$.
- If T is a Fredholm operator, the adjoint T^* is also Fredholm, and $index(T^*) = -index(T)$.

Theorem 8.2 (Fredholm Alternative) *Consider a compact operator $T : X \to X$, and $\lambda \in \mathbb{C}$ non-zero. Only one of the following statements hold true:*

(i) Equation $Tu = \lambda u$ has a non-trivial solution $u \in X$;
(ii) The operator $T - \lambda$ has a bounded inverse $(T - \lambda)^{-1}$ on X.

The second statement is equivalent to the fact that the non-homogeneous equation $Tu = \lambda u - f$ has a unique solution for each $f \in X$. One can prove the Fredholm alternative using the index theory of Fredholm operators (by showing that $index(T - \lambda) = 0$, which implies that $T - \lambda$ is surjective whenever there is no eigenvalue).

Moreover, the Fredholm alternative can be restated in terms of Fredholm indices [43]: if K is a compact operator and $\lambda \neq 0$, then $\lambda I - K$ is Fredholm, and $index(\lambda I - K) = 0$

It should be mentioned that the Fredholm alternative can be used to establish spectral results for compact operators. Note that the spectrum of an operator T is

defined as [43]:

$$\sigma(T) = \{\lambda \in \mathbb{C} | \lambda I - T \text{ is not invertible}\}.$$

Buono and Eftimie [30] showed that for the nonlocal hyperbolic systems (5.14), the operator $T = \frac{d}{dt} - \mathscr{L}$ (with $\mathscr{L}$ the linearised operator at a steady state $u_*(x)$) is a Fredholm operator of index zero. It was also proven that the spectrum of $\mathscr{L}$ is made up of a finite number of eigenvalues with finite multiplicity [30]. This result ensures that the Centre Manifold Theorem (see Sect. 8.6) holds for this class of nonlocal hyperbolic systems (5.14).

8.5 Analytical Approaches for the Investigation of Patterns: Weakly Nonlinear Analysis

The method of weakly nonlinear analysis generalises the linear stability analysis performed near a bifurcation point, by including also nonlinear terms (via an asymptotic expansion). As discussed above, the linear stability analysis is valid only for small time and infinitesimal perturbations, and cannot capture the long-time effect of the nonlinear terms which dominate the growth of the unstable modes. To overcome this impediment, the weakly nonlinear analysis uses two separate time scales: a fast time scale described by the original time variable t (which gives the time region where the solution starts to develop), and a slow time scale ($T = \epsilon^m t$, for some $m > 0$) on which the effects of the nonlinear terms become important. (Note that close to the bifurcation point, the amplitude of the patterns evolves on a slow temporal scale.) It is assumed that as $\epsilon \to 0$, the two time variables (t and T) are independent. The weakly nonlinear analysis then reduces the dynamics of the full system to the temporal evolution (on the slow time scale) of the amplitude of the perturbations of the steady state, and these differential equations (either ODEs or PDEs) are faster to solve than the full nonlinear systems.

Although the weakly nonlinear analysis can be performed in the neighborhood of codim-1 [44] and codim-2 points [27, 28], in the following we focus on the simpler case of codimension-1 bifurcations (with real eigenvalues) and describe the main steps of this approach. To this end, we consider the 1D nonlocal hyperbolic system (5.14) introduced in [14, 44], which can exhibit codimension-1 steady-state bifurcations as we vary, for example, the magnitude of attractive interactions q_a. Denote by q_a^* the critical value of q_a for which the dispersion relation satisfies $\sigma(q_a^*, k_c) = 0$ (where $k = k_c > 0$ is the critical wavenumber; e.g., $k_c = k_2$ in Fig. 8.2a for the dispersion relation described by the dotted curve). A solution of (5.14) near the bifurcation point is given by (see [44])

$$u^{\pm}(x,t) \propto e^{\sigma t + i k_c x} + \text{c.c.}, \tag{8.29}$$

where "c.c" stands for "complex conjugate". Perturbing the parameter q_a in the neighborhood of its critical value, $q_a = q_a^* + \nu\epsilon^2$ (with $0 < \epsilon \ll 1$ and $\nu = \pm 1$ a parameter that will give the direction of the bifurcating solution branches), substituting this expression into the dispersion relation $\sigma(q_a, k_c)$ and expanding it into Taylor series about q_a^* leads to the following eigenfunction for the solution:

$$e^{\sigma(q_a,k_c)t+ik_cx} \approx e^{ik_cx+\sigma(q_a^*,k_c)+\frac{d\sigma(q_a^*,k_c)}{dq_a}} = e^{ik_cx+\frac{d\sigma(q_a^*,k_c)}{dq_a}} = \alpha(\epsilon^2 t)e^{ik_cx}. \tag{8.30}$$

Since the amplitude of the solution depends on the slow time $\epsilon^2 t$, the authors in [44] introduced a slow-time variable $T = \epsilon^2 t$. The left-moving and right-moving densities were re-written as $u^{\pm}(x,t) = \tilde{u}^{\pm}(x,t,\epsilon,T)$. After dropping the tilde for simplicity and assuming a formal expansion of $u^{\pm}$ in powers of ϵ,

$$u^+(x,t,\epsilon,T) = u_*^+ + \epsilon u_1^+ + \epsilon^2 u_2^+ + \epsilon^3 u_3^+ + O(\epsilon^4),$$
$$u^-(x,t,\epsilon,T) = u_*^- + \epsilon u_1^- + \epsilon^2 u_2^- + \epsilon^3 u_3^- + O(\epsilon^4),$$

these expressions can be substituted into the nonlinear system (5.14). The nonlinear turning rates $\lambda^{\pm}[u^+, u^-]$ are then expanded in Taylor series about the steady states $u_*^{\pm}$. Overall, the nonlinear hyperbolic system (5.14) can be re-written as

$$0 = N\Big(\sum_{j\geq 1}\epsilon^j u_j\Big) \approx \sum_{j\geq 1}(\mathscr{L}(u_j) + \mathscr{N}_j(u_{j-k}) + \mathscr{E}_j), \quad k \geq 1. \tag{8.31}$$

Here, $\mathscr{L}(u_j)$ describes the linear part of the system (5.14), $\mathscr{N}_j(u_{j-k})$ contains nonlinear terms formed of $u_{j-1}^{\pm}$, $u_{j-2}^{\pm}$, etc. (which were calculated at previous $O(\epsilon^{j-k})$ steps, where $k \geq 1$), and $\mathscr{E}_j$ contains the slow time derivatives $\partial_T u_{j-2}^{\pm}$ (for $j \geq 3$) and the terms multiplied by ν. While the linear operator $\mathscr{L}$ is the same at each $O(\epsilon^j)$, the nonlinear operators $\mathscr{N}_j$ and $\mathscr{E}_j$ are calculated at each j-step. For the nonlocal system (5.14) described in [44], the linear operator $\mathscr{L}$ is given by

$$\mathscr{L}(u) = \begin{pmatrix} \gamma\partial_x + L_1 + M_5 K \star \cdot & -L_1 + M_5 K \star \cdot \\ -L_1 - M_5 K \star \cdot & -\gamma\partial_x + L_1 - M_5 K \star \cdot \end{pmatrix} \begin{pmatrix} u^+ \\ u^- \end{pmatrix}, \tag{8.32}$$

where L_1 and M_5 are constants depending on the steady states and the various model parameters, while the convolutions "$K\star\cdot$" are defined as a difference between repulsive and attractive nonlocal interactions:

$$K \star u^{\pm} = q_r\big(\tilde{K}_r \star u^{\pm} - K_r \star u^{\pm}\big) - q_a^*\big(\tilde{K}_a \star u^{\pm} - K_a \star u^{\pm}\big), \tag{8.33}$$

with $\tilde{K}_{r,a}(s) = K_{r,a}(-s)$ and $K_{r,a} \star u^{\pm}(x) = \int_{-\infty}^{\infty} K_{r,a}(s)u^{\pm}(x-s)ds$.

At $O(\epsilon^1)$ the nonlinear terms are zero ($\mathscr{N}_1 = \mathscr{E}_1 = 0$), and solving the nonlinear system (5.14) reduces to solving the linear system $\mathscr{L}(u) = 0$, which has a nontrivial solution. For this reason, at each $O(\epsilon^j)$, $j \geq 2$, the nonlinear system $\mathscr{L}(u_j) =$

$\mathscr{N}_j + \mathscr{E}_j$ has a solution if and only of $\mathscr{N}_j + \mathscr{E}_j$ satisfies the Fredholm alternative. To check whether this alternative is applied, one needs to investigate first whether the linear operator $\mathscr{L}$ is compact. Consider the Hilbert space [44]

$$Y = \{\mathbf{v}(x,t) \in [0,L] \times [0,\infty) | \lim_{T\to\infty} \frac{1}{T} \int_0^T \int_0^L |\mathbf{v}|^2 dx dt < \infty\} \tag{8.34}$$

with the inner product

$$\langle \mathbf{v}, \mathbf{w} \rangle = \lim_{T\to\infty} \int_0^T \int_0^{L=2\pi/k_c} \left(v^1 \bar{w}^1 + v^2 \bar{w}^2\right) dx dt. \tag{8.35}$$

Here $\mathbf{v} = (v^1, v^2)^\top$ and $\mathbf{w} = (w^1, w^2)^\top$, which satisfy periodic boundary conditions. Since $\mathbf{v}$ are bounded on $L^2([0,L] \times [0,T])$ (see [44]), then $\lim_{T\to\infty}(1/T)||\mathbf{v}||^2_{L^2([0,L]\times[0,T])}$ is finite. Because the linear operator $\mathscr{L}$ is given also in terms of the differential operator $\partial/\partial x$ (which is not bounded), one needs to interpret this differential operator as a distribution in a Sobolev subspace of Y. Consider the space

$$V_{bc} = \{(v^+, v^-) \in Y | (\partial_x v^+, \partial_x v^-) \in Y, \text{ and } v^\pm(L,t) = v^\pm(0,t)\}, \tag{8.36}$$

with the norm $||v||^2_{V_{bc}} = ||(v^+, v^-)||^2_Y + ||(\partial_x v^+, \partial_x v^-||^2_Y$, which is associated with the inner product (8.35). As discussed in [27], the linear operator $\mathscr{L} : V_{bc} \to Y$ is bounded, and following the approach in Kmit and Recke [45] for linear local hyperbolic systems, one can show that $\mathscr{L}$ is a Fredholm operator; see the proof for nonlocal hyperbolic systems in [30].

Since the Fredholm alternative can be applied, the term $\mathscr{N}_j + \mathscr{E}_j$ has to be orthogonal on the bounded solution of the adjoint homogeneous problem $\mathscr{L}^*(\hat{u}) = 0$:

$$\langle \hat{u}, \overline{(\mathscr{N}_j + \mathscr{E}_j)} \rangle = 0. \tag{8.37}$$

Focusing only on those terms in $\mathscr{N}_j + \mathscr{E}_j$ that contain the exponentials $e^{\pm i k_c x}$ (since they give rise to secular solutions that grow unbounded), and substituting these terms into the inner product (8.37) one eventually obtains the following differential equation for the evolution of the amplitude $\alpha(T)$ (truncated here at the third order $\alpha|\alpha|^2$):

$$\frac{d\alpha}{dT} = -\nu\alpha Y - \alpha|\alpha|^2 X, \tag{8.38}$$

where X and Y are constant terms that depend on model parameters. This complex amplitude can be re-written as $\alpha(T) = R(t)e^{i\theta(T)}$, with real terms $R(T) = |\alpha|$ and

$\theta(T)$ that satisfy

$$\frac{dR}{dT} = -\nu R\Re(Y) - R^3\Re(X), \tag{8.39}$$

$$\frac{d\theta}{dT} = -\nu\Im(Y) - R^3\Im(X). \tag{8.40}$$

Here $\Im$ and $\Re$ denote the imaginary and real parts of the coefficients X and Y. The equation for the real amplitude $R(T)$ exhibits two steady states: $R = 0$ and $R = \sqrt{-\nu\Re(Y)/\Re(X)}$. The stability of these states can be investigated in a classical way via small perturbations: $R(T) = R^* + R_\delta$, with R^* denoting the steady state and R_δ being a small perturbation which satisfies

$$\frac{dR_\delta}{dT} = R_\delta\big(-\nu\Re(Y) - 2R^{*2}\Re X\big). \tag{8.41}$$

It is easy to observe that the zero state $R^* = 0$ is stable for $\nu\Re(Y) > 0$ and unstable otherwise. In contrast, the nonzero state $R^* = \sqrt{-\nu\Re(Y)/\Re(X)}$ is stable for $\nu\Re(Y) < 0$ and unstable otherwise. One can graph the solution of (8.39) (and its stability) for the exact parameter values used during numerical simulations, to obtain bifurcation diagrams for the amplitudes of the solution branches as functions of parameter values (e.g., q_a here). We graph two caricature examples of the bifurcating branches in Fig. 8.7 (see also Fig. 5.9 for bifurcation diagrams based on specific model parameters, as we vary the magnitude of alignment q_{al}).

Remark 8.4 Note in Fig. 8.7a that the 3rd-order truncation of the amplitude equation (8.38) allows only for the detection of the main nontrivial amplitude branch that bifurcates from $\alpha = 0$ at $q_a = q_a^*$. The fact that this branch is unstable, it suggests that there exists also a stable high-amplitude spatially heterogeneous solution towards which the small perturbations of the spatial homogeneous steady state will grow, and which can be detected numerically. Therefore, in the range $q_a \in (q^*, q_a^*]$ two qualitatively different stable states co-exit (together with an unstable state). One could identify the secondary bifurcation point $q_a = q^*$ where the unstable branch $\alpha > 0$ changes stability and becomes stable by considering truncations of (8.38) up to the 5th and even 7th orders.

Remark 8.5 We also note in Fig. 8.7a a *hysteresis phenomenon* characterised by a lack of reversibility in the dynamics of the system: for $q_a > q_a^*$ the zero-amplitude ($\alpha = 0$) solution is unstable and small perturbations of it will grow and give rise to high-amplitude spatially heterogeneous solutions (i.e., the solution jumps fast to the upper red curve). As we decrease q_a below q_a^* the dynamics of the system follows the stable high-amplitude branch, and does not decrease immediately to $\alpha = 0$. The solution jumps back to $\alpha = 0$ only when $q_a = q^*$. The bifurcation at $q_a = q^*$ is a saddle-node bifurcation. Moreover, the high-amplitude state exists only for $q_a > q^*$. It could be possible that for some very large q_a (i.e., q_a further away from the bifurcation point q_a) this high-amplitude state disappears through a

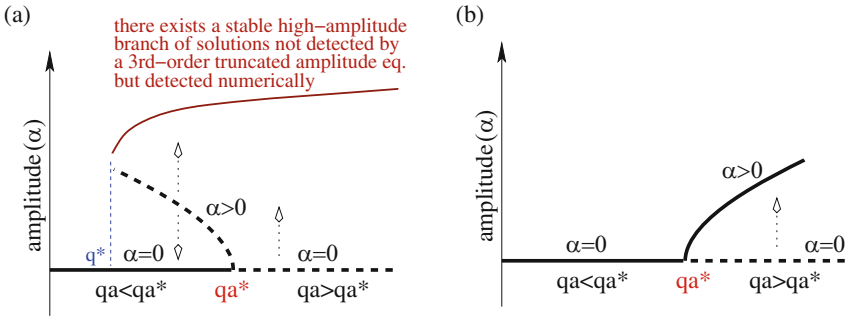

Fig. 8.7 Caricature description of the bifurcation diagram near a codimension-1 bifurcation point, in the (α, q_a) plane. The continuous curves describe the stable states and the dashed curves describe the unstable states. (**a**) Subcritical bifurcation obtained for $\nu < 0$: for $q_a < q_a^*$ small perturbations of the homogeneous steady state (with zero amplitude) decay to zero, while large perturbations (above the nonzero dashed curve) growth even larger towards a high-amplitude spatially heterogeneous solution (which is detected numerically). At the point $q_a = q^*$ (usually located further away from the bifurcation point q_a^*) the unstable branch $\alpha > 0$ becomes unstable through a saddle-node bifurcation. For $q_a > q_a^*$ small perturbations of the homogeneous steady state grow towards a high-amplitude heterogeneous state. (**b**) Supercritical bifurcation obtained for $\nu > 0$: for $q_a > q_a^*$ small perturbations grow and give rise to a small-amplitude spatially heterogeneous solution, while for $q_a < q_a^*$ the small perturbations decay towards zero as the homogeneous steady state is stable

different bifurcation; however, this aspect cannot be investigated through a weakly nonlinear analysis which loses its validity away from the bifurcation points.

Weakly nonlinear analysis has been applied to investigate the solutions emerging in the vicinity of other bifurcation points [27, 28, 44]:

- a Hopf bifurcation point [44], where $\sigma := \pm i\omega$ and the solution can be represented as

$$u^{\pm}(x, t, T) \propto \beta(T) e^{i\omega t + i k_c x} + \text{c.c.} \tag{8.42}$$

The equation for the variation of amplitude $\beta(T)$ on the slow time scale T is similar to the one for the steady-state bifurcation point (8.38):

$$\frac{d\beta(T)}{dT} = -\beta Y - \beta|\beta|^2 X, \tag{8.43}$$

with X and Y given in terms of the model parameters. If we now take into consideration also the reflection symmetry of the domain, we can represent the solution as

$$u^{\pm}(x, t, T) \propto \beta_1(T) e^{i\omega t + i k_c x} + \beta_2(T) e^{i\omega t - i k_c x} + \text{c.c.} \tag{8.44}$$

In this case, the equations for the variation of the amplitudes $\beta_1(T)$ and $\beta_2(T)$ are

$$\frac{d\beta_1(T)}{dT} = -\beta_1 X_1 + \beta_1|\beta_1|^2 X_2 + \beta_1|\beta_2|^2 X_3, \tag{8.45a}$$

$$\frac{d\beta_2(T)}{dT} = -\beta_2 Y_1 + \beta_2|\beta_1|^2 Y_2 + \beta_2|\beta_2|^2 Y_3. \tag{8.45b}$$

Note that by considering also the reflection symmetry, we obtain a system of coupled normal form equations, which exhibits more complex steady states compared to Eq. (8.43).

- a Hopf/Hopf bifurcation point [27], where the solution can be represented as (considering also the reflection symmetry of the domain):

$$\begin{aligned} u^{\pm}(x,t) \propto\ & \alpha_1(T)e^{i\omega(k_m)t+ik_m x} + \alpha_2(T)e^{i\omega(k_m)t-ik_m x} + \beta_1(T)e^{i\omega(k_n)t+ik_n x} \\ & +\beta_2(T)e^{i\omega(k_n)t-ik_n x} + \text{c.c.}, \end{aligned} \tag{8.46}$$

with $k_m \neq k_n$ the two distinct Hopf interacting modes. The equations for the variation of the amplitudes on the slow-time scale T are given as follows:

$$\begin{aligned} \frac{d\alpha_1(T)}{dT} &= -\alpha_1 X_1 + \alpha_1|\alpha_1|^2 X_2 + \alpha_1|\alpha_2|^2 X_3 + \alpha_1|\beta_1|^2 X_4 + \alpha_1|\beta_2|^2 X_5, \\ \frac{d\alpha_2(T)}{dT} &= -\alpha_2 Y_1 + \alpha_2|\alpha_1|^2 Y_2 + \alpha_2|\alpha_2|^2 Y_3 + \alpha_2|\beta_1|^2 Y_4 + \alpha_2|\beta_2|^2 Y_5, \\ \frac{d\beta_1(T)}{dT} &= -\beta_1 Z_1 + \beta_1|\alpha_1|^2 Z_2 + \beta_1|\alpha_1|^2 Z_3 + \beta_1|\beta_1|^2 Z_4 + \beta_1|\beta_2|^2 Z_5, \\ \frac{d\beta_2(T)}{dT} &= -\beta_2 \Psi_1 + \beta_2|\alpha_1|^2 \Psi_2 + \beta_2|\alpha_2|^2 \Psi_3 + \beta_2|\beta_1|^2 \Psi_4 + \beta_2|\beta_2|^2 \Psi_5. \end{aligned}$$

The symmetries of the model lead to similarities between the parameters X_i, Y_i, Z_i and Ψ_i, $i = 1, \ldots, 5$:

$$\begin{aligned} & X_1 = Y_1, \quad Z_1 = \Psi_1, \quad X_2 + X_3 = Y_2 + Y_3, \quad Z_2 + Z_3 = \Psi_2 + \Psi_3, \\ & X_4 + X_5 = Y_4 + Y_5, \quad Z_4 + Z_5 = \Psi_4 + \Psi_5. \end{aligned}$$

Since these similarities in parameter values mean that the steady state solutions have conjugate isotropy subgroups, it allowed the authors in [27] to ignore some of the solutions of the above system of coupled amplitude equations. We summarise in Table 8.1 the various types of solutions that emerge near a Hopf/Hopf bifurcation point (given in terms of the above amplitudes) and their corresponding isotropy subgroups; for details see [27].

- a Hopf/Steady-state bifurcation point [28], where the solution can be represented as (considering also the reflection symmetry):

$$u^{\pm}(x,t) \propto \alpha(T)e^{ik_m x} + \beta_1(T)e^{i\omega(k_n)t+ik_n x} + \beta_2(T)e^{i\omega(k_n)t-ik_n x} + \text{c.c}, \tag{8.47}$$

  with k_m the steady-state mode and k_n the Hopf mode. The equations for the variation of the amplitudes on the slow-time scale T are

$$\begin{aligned}
\frac{d\alpha}{dT} &= -\alpha X_1 + \alpha|\alpha|^2 X_2 + \alpha|\beta_1|X_3 + \alpha|\beta_2|^2 X_4,\\
\frac{d\beta_1}{dT} &= -\beta_1 Y_1 + \beta_1|\alpha|^2 Y_2 + \beta_1|\beta_1|^2 Y_3 + \beta_1|\beta_2|^2 Y_4,\\
\frac{d\beta_2}{dT} &= -\beta_2 Z_1 + \beta_2|\alpha|^2 Z_2 + \beta_2|\beta_2|^2 Z_3 + \beta_2|\beta_1|^2 Z_4.
\end{aligned}$$

  Parameters X_i, Y_i, Z_i, $i = 1, .., 4$, depend on model parameters, and are related through the symmetries of the system [28].
- a steady-state/steady-state bifurcation point [28], where the solution can be represented as

$$u^{\pm}(x,t) \propto \alpha_1(T)e^{ik_m x} + \alpha_2(T)e^{ik_n x} + \text{c.c}, \tag{8.48}$$

  with k_m and k_n the two distinct steady-state modes. The equations for the evolution of the amplitudes are

$$\begin{aligned}
\frac{d\alpha_1(T)}{dT} &= -\alpha_1 X_1 + \alpha_1|\alpha_1|^2 X_2 + \alpha_1|\alpha_2|^2 X_3,\\
\frac{d\alpha_2(T)}{dT} &= -\alpha_2 Y_1 + \alpha_2|\alpha_1|^2 Y_2 + \alpha_2|\alpha_2|^2 Y_3.
\end{aligned}$$

Remark 8.6 We need to discuss briefly the normal form equation (8.38) (and implicitly the coupled systems of normal form equations given above). In general, one assumes that the amplitude α depends not only on the slow time scale T but also on a slow space variable $X = \epsilon^p x$. This leads to a PDE (i.e., a Ginzburg-Landau amplitude equation) for the evolution of $\alpha(X, T)$. However, for the nonlocal hyperbolic system (5.14) with periodic boundary conditions, the zero mode $k = 0$ is not an admissible mode (due to the conservation of the total density, which is not satisfied by eigenfunctions with modes $k = 0$ on finite domains with periodic boundary conditions). In this case, one could assume that $\alpha = \alpha(T)$ and the temporal evolution of the amplitude is reduced to an ODE (8.38) (i.e., a Stuart-Landau amplitude equation).

However, since numerical simulations for these nonlocal hyperbolic models have shown the existence of patterns with space-modulated amplitudes (see the semi-zigzags and travelling breathers in Fig. 5.7f, i) it would be interesting to investigate

the evolution of the space-modulated amplitude equation ($\alpha(X, T)$) on infinite domains.

8.6 Centre Manifold Theory

We have seen in Sect. 8.5 that the multiple scales approach for the weakly nonlinear analysis reduces the infinite-dimensional PDE system (5.14) to a finite-dimensional ODE system that can be investigated more easily (and which preserves the stability and bifurcation structure of the original system). Other approaches that can be used to reduce the hyperbolic and kinetic equations/systems to more manageable equations/systems are the Centre Manifold reduction and the Lyapunov-Schmidt reduction. The Centre Manifold reduction focuses on finding a dynamical subsystem invariant under the flow of the full system (and which contains the bifurcation that needs to be investigated), while the Lyapunov-Schmidt reduction focuses on identifying an equation for the equilibria (fixed points or periodic solutions), and then performing a reduction of this equation to a low-dimension set of algebraic equations (also called the bifurcation equations) [46]. A review of these two approaches in the context of nonlocal hyperbolic systems can be found in [30]. Note that the Fredholm property of the linear operator $\mathscr{L}$, which we discussed in Sects. 8.4 and 8.5, is central to the application of the Lyapunov-Schmidt reduction; see [30]. However, in the following we will ignore the Lyapunov-Schmidt reduction, and focus only on the Centre Manifold reduction. For a detailed presentation of the Lyapunov-Schmidt reduction in both finite and infinite dimensions, we refer the reader to [46].

Mirroring the approach in Sect. 8.1 (where we first looked at linear stability results in ODE systems and then in PDE systems), here too we start our discussion on the Centre Manifold Theorem (which ensures the possibility of having a Centre Manifold reduction to simplify the model dynamics around a non-hyperbolic fixed point) by focusing first on the finite-dimensional systems. Then, we consider its generalisation to infinite-dimensional systems. This approach allows us to show how the classical, simple version of the theorem that is listed in almost all books on dynamical systems and bifurcation theory [6, 9], is generalised to infinite dimensions through the addition of some extra assumptions.

- **Finite-dimensional systems.** In the following we give the statement of the Centre Manifold Theorem for ODE systems. We also discuss the form of the extended centre manifold, which includes also a dependence on parameters and thus can be used for bifurcation results. But first let us define the stable, unstable and centre subspaces of a linear system $du/dt = Au$. To this end, assume that matrix A has eigenvalues $\lambda_j = a_j + ib_j$, and corresponding to these eigenvalues there are the generalised eigenvectors $w_j = w_j^1 + iw_j^2$. Then the stable (E^s), unstable (E^u) and centre (E^c) subspaces spanned by the real and imaginary parts

of the eigenvectors w_j corresponding to eigenvalues λ_j are:

$$E^s = Span\{w_j^1, w_j^2 | a_j < 0\},$$
$$E^u = Span\{w_j^1, w_j^2 | a_j > 0\},$$
$$E^c = Span\{w_j^1, w_j^2 | a_j = 0\}.$$

Theorem 8.3 (Centre Manifold Theorem [9]) *Consider the nonlinear system*

$$\frac{du}{dt} = f(u), \quad u \in \mathbb{R}^n, \tag{8.49}$$

with $f \in C^r(E)$, $r \geq 1$, and $E \subset \mathbb{R}^n$ which includes the origin. Assume that $f(0) = 0$, and $Df_u(0)$ has p eigenvalues with positive real parts, k eigenvalues with negative real parts, and $m = n - p - k$ eigenvalues with zero real parts. Then there exists a m-dimensional centre manifold $W^c(0)$ tangent to the centre subspace E^c at 0, a k-dimensional stable manifold $W^s(0)$ tangent to the stable subspace E^s at 0, and a p-dimensional unstable manifold $W^u(0)$ tangent to the unstable subspace E^u at 0.

Locally, system (8.49) can be written as

$$\frac{du}{dt} = Cu + F(u, v), \quad \frac{dv}{dt} = Pv + G(u, v), \tag{8.50}$$

with $(u, v) \in \mathbb{R}^m \times \mathbb{R}^{k+p}$, C is a square matrix with m eigenvalues with zero real parts, and P is a square matrix with k eigenvalues with negative real parts and p eigenvalues with positive real parts. Moreover, $F(0) = G(0) = 0$, $DF(0) = DG(0) = 0$, and there is a function $h(u) = v$ (that defines the central manifold) such that the flow on the central manifold is given (locally, for $|u| < \delta$) by

$$\frac{du}{dt} = Cu + F(u, h(u)), \quad \text{for all } u \in \mathbb{R}^m \text{ with } |u| < \delta. \tag{8.51}$$

In the context of bifurcation theory, we need to consider also the effect of a parameter μ. For this reason, we work on *extended central manifolds*, where we generalise Eq. (8.50) through the addition of a trivial equation for the derivative of parameter μ:

$$\frac{du}{dt} = Cu + F(u, v, \mu), \quad \frac{dv}{dt} = Pv + G(u, v, \mu), \quad \frac{d\mu}{dt} = 0. \tag{8.52}$$

We note that the equation for the derivative of μ adds one more dimension to the centre manifold ($= m + 1$), since now we work in the neighbourhood of $(u, v) = (0, 0)$ and $\mu = 0$ (where the bifurcation occurs). Moreover, the equation that parametrises the centre manifold now has the form $v = h(u, \mu)$. Therefore,

the equation for the extended central manifold can be written as

$$\frac{du}{dt} = Cu + F(u, h(u, \mu), \mu). \tag{8.53}$$

If u is a scalar and $C = 0$, then the above equation can have three possible descriptions, corresponding to the saddle-node, transcritical and pitchfork bifurcations discussed in Sect. 8.2:

$$\text{Saddle-node:} \quad \frac{du}{dt} = \mu + cu^2,$$
$$\text{Transcritical:} \quad \frac{du}{dt} = \mu u + cu^2,$$
$$\text{Pitchfork:} \quad \frac{du}{dt} = \mu u + cu^3.$$

For a detailed proof of the Centre Manifold Theorem, we refer the reader to [9, 47].

- **Infinite-dimensional systems.** The centre manifold theory for PDEs has been developed in various studies published over the past three decades (see [5, 48–51] and the references therein). In the following we give the assumptions and the statement of the Centre Manifold Theorem for infinite-dimensional systems (following the approach in [5]), and then discuss the applicability of this theorem to the class of nonlocal 1D hyperbolic systems (5.14) discussed in Chap. 5.

  First, let us consider three Banach spaces, X, Y and Z, which satisfy the following continuous embeddings:

$$Z \hookrightarrow Y \hookrightarrow X. \tag{8.54}$$

We define $\mathbb{L}(Z, X)$ to be the Banach space of linear bounded operators $\mathscr{L} : Z \to X$, with the operator norm

$$||\mathscr{L}||_{\mathbb{L}(Z,X)} = \sup_{||u||_Z=1} (||\mathscr{L}u||_X) \tag{8.55}$$

For some $k \geq 2$ we define $\mathscr{C}^k(Z, X)$ the Banach space of functions $b : Z \to X$ that are k-times continuously differentiable. The space is equipped with the following norm:

$$||b||_{\mathscr{C}^k} = \max_{j=0,\ldots,k} \left(\sup_{y\in Z} ||D^j b(y)||_{\mathbb{L}(Z^j,X)} \right), \tag{8.56}$$

where D denotes the differential operator. Finally, for a constant $\eta > 0$, we define the space $\mathscr{C}_\eta(\mathbb{R}, X)$ of exponentially growing functions with the norm

$$||u||_{\mathscr{C}_\eta} = \sup_{t\in\mathbb{R}} \left(e^{-\eta|t|} ||u(t)||_X \right) < \infty, \quad \text{for } u \in \mathscr{C}^0(\mathbb{R}, X). \tag{8.57}$$

Assume now that a generic PDE can be represented as

$$\frac{du}{dt} = F(u) = \mathscr{L}u + \mathscr{N}(u). \tag{8.58}$$

Here $\mathscr{L}$ and $\mathscr{N}$ are the linear and nonlinear parts of operator F. Next, we list the hypotheses that need to be satisfied by $\mathscr{L}$ and $\mathscr{N}$ for the existence of a central manifold, as given in [5]:

(A) Assume that $\mathscr{L} \in \mathbb{L}(Z, X)$, and for some $k \geq 2$ there exist a neighborhood $\mathscr{V}(0)$ of 0 such that $\mathscr{N} \in \mathscr{C}^k(\mathscr{V}, Y)$ and $\mathscr{N}(0) = 0$ (i.e., $u = 0$ is an equilibrium of (8.58)) and $D\mathscr{N}(0) = 0$ (i.e., $\mathscr{L}$ is the linearisation of the operator $\mathscr{N}$ about 0).

(B) Consider the spectrum σ of the linear operator $\mathscr{L}$, which is defined as $\sigma = \sigma_+ \bigcup \sigma_0 \bigcup \sigma_-$, with

$$\sigma_+ = \{\lambda \in \sigma | Re(\lambda) > 0\},\ \sigma_0 = \{\lambda \in \sigma | Re(\lambda) = 0\},$$
$$\sigma_- = \{\lambda \in \sigma | Re(\lambda) < 0\}.$$

Assume that there is a positive constant $g > 0$ such that

$$\inf_{\lambda \in \sigma_+} (Re\lambda) > g \quad \text{and} \quad \sup_{\lambda \in \sigma_-} (Re\lambda) < -g. \tag{8.59}$$

Moreover, assume that the set σ_0 has a finite number of eigenvalues with finite algebraic multiplicities.

(C) Let P_0 be the projection onto the generalised eigenspaces of σ_0, and define $P_h = I - P_0$. Consider now the linear operator $\mathscr{L}_h$ which is the restriction of $\mathscr{L}$ to $d(\mathscr{L})_h = P_h D(\mathscr{L})$. Then, for any $\eta \in [0, g]$ and any $f \in \mathscr{C}_\eta(\mathbb{R}, Y_h)$, the linear problem

$$\frac{du_h}{dt} = \mathscr{L}_h u_h + f(t) \tag{8.60}$$

has a unique solution $u_h = K_h f \in \mathscr{C}(\mathbb{R}, Z_h)$, with K_h a bounded linear operator from $\mathscr{C}_\eta(\mathbb{R}, Y_h)$ to $\mathscr{C}_h(\mathbb{R}, Z_h)\big)$. Also, there exist a continuous map $\mathscr{C} : [0, g] \to \mathbb{R}$ such that

$$||K_h||_{\mathbb{L}\left(\mathscr{C}_\eta(\mathbb{R}, Y_h), \mathscr{C}_h(\mathbb{R}, Z_h)\right)} \leq C(\eta). \tag{8.61}$$

Theorem 8.4 (Centre Manifold Theorem [5]) *Assume that hypotheses (A)–(C) hold. Then there exist a map $\Psi \in \mathscr{C}^k(\mathscr{E}_0, Z_h)$ with $\Psi(0) = 0$, $D\Psi(0) = 0$, and a neighborhood of 0, $\mathscr{O}(0) \in Z$ such that the manifold*

$$\mathscr{M}_0 = \{u_0 + \Psi(u_0),\ \textit{for } u_0 \in \mathscr{E}_0\} \subset Z \tag{8.62}$$

satisfies the following conditions:

(i) $\mathscr{M}_0$ *is locally invariant;*
(ii) $\mathscr{M}_0$ *contains the set of bounded solutions of (8.58) that stay in* $\mathscr{O}$ *for all* $t \in \mathbb{R}$.

Here, the manifold $\mathscr{M}_0$ is called a *local centre manifold*, while the map Ψ is called the *reduction function*.

If we consider now a solution u of (8.58), with $u \in \mathscr{M}_0$, then we can write $u = u_0 + \Psi(u_0)$, with u_0 satisfying

$$\frac{du_0}{dt} = \mathscr{L}_0 u_0 + P_0 \mathscr{N}(u_0 + \Psi(u_0)). \tag{8.63}$$

Here, $\mathscr{L}_0$ is the restriction of $\mathscr{L}$ to $\mathscr{E}_0 = Range(P_0) = \{P_0 u \in X | u \in Z\}$.

As for the finite-dimensional case, let us consider a parameter-dependent PDE,

$$\frac{du}{dt} = F(u) = \mathscr{L}u + \mathscr{N}(u, \mu), \tag{8.64}$$

with $\mathscr{N}(u, \mu)$ defined in the neighborhood of $(0, 0) \in Z \times \mathbb{R}^m$. Then we obtain an analogue of the previous Centre Manifold Theorem, with the parameter-dependent local extended centre manifold given by [5]:

$$\mathscr{M}_0(\mu) = \{u_0 + \Psi(u_0, \mu), \text{ for } u_0 \in \mathscr{E}_0\} \subset Z. \tag{8.65}$$

To understand better the difficulties of applying this theorem to hyperbolic systems, let us first give the following spectral property.

Definition 8.16 (Spectral Mapping Property [52]) Consider A an infinitesimal generator of a C_0 semigroup e^{At}. Then A has the *spectral mapping property* if the spectrum of this semigroup, $\sigma(e^{At})$, satisfies:

$$\sigma(e^{At}) \setminus \{0\} = \overline{e^{\sigma(A)t}} \setminus \{0\}, \text{ for } t \geq 0, \tag{8.66}$$

where $\overline{e^{\sigma(A)t}}$ denotes the closure of the set.

It was shown by Renardy [53] that for hyperbolic systems the spectral mapping property does not generally hold (see also the dispersion relation shown in Fig. 4.7, for the local hyperbolic system introduced in [15]). This impacts the validity of the Central Manifold theorems for hyperbolic systems (since the hypothesis (B) given above is violated). Lichtner [52] has proven that this spectral property holds for a class of linear hyperbolic systems. Moreover, different versions of the Central Manifold Theorem were proven for various

(local) hyperbolic systems with applications to fluid dynamics or lasers [54–56]. Returning to the class of nonlocal 1D hyperbolic models (5.14) introduced in Chap. 5, it was shown in [30] that if $u^{**}(x)$ is a steady state solution of the nonlocal hyperbolic system (5.14) and $\mathscr{L}$ is the linearised operator at $u^{**}(x)$, then the spectrum of $\mathscr{L}$ contains isolated eigenvalues with finite multiplicity and no accumulation point in $\mathbb{C}$. Moreover, this spectrum has only a finite number of eigenvalues with finite multiplicity on the imaginary axis [30], and thus hypothesis (B) holds true. Using the model symmetries to decompose (5.14) into a family of finite-dimensional systems, it was shown in [30] that also hypothesis (C) was satisfied.

We emphasise that the validity of the spectral property for the various hyperbolic/kinetic models discussed throughout this monograph is still an open problem.

We conclude this section by giving the statement of the Contraction Mapping Theorem (which is used in the construction of the Centre Manifold [47], or in the proof of existence of unique solutions for hyperbolic systems—as mentioned in Chap. 4). To this end, we use the version of the theorem stated in [47].

Theorem 8.5 (Contraction Mapping Theorem [47]) *Consider two Banach spaces X and Y, and a continuous map $F : X \times Y \to Y$ that is a contraction in the second variable:*

$$||F(x, y) - F(x, y')|| \leq k||y - y'||, \quad \forall\, x \in X,\ \forall\, y, y' \in Y, \quad \text{and some } k < 1.$$

The following results hold true:

1. *For every $x \in X$, there exists a unique fixed point $y(x) \in Y$ for the map F:*

$$y(x) = F(x, y(x)).$$

2. *For every $x \in X$, $y \in Y$, the following inequality holds true:*

$$||y - y(x)|| \leq \frac{1}{1-k}||x - x'||.$$

3. *If the map F is Lipschitz continuous with respect to x,*

$$||F(x, y) - F(x', y)|| \leq L||x - x'||, \quad \forall x, x' \in X,\ \forall y \in Y,$$

then the map $x \to y(x)$ is also Lipschitz continuous with respect to x:

$$||y(x) - y(x')|| \leq \frac{L}{1-k}||x - x'||.$$

4. *For any convergent sequence* $x_n \to \bar{x} \in X$*, and any* $y_0 \in Y$*, the sequence of iterates* $y_{n+1} = F(x_n, y_n)$ *converges to the fixed point* $\bar{y} = y(\bar{x})$.

For a proof of this theorem see [47].

8.7 Stochastic Bifurcations

As we have seen numerically at the end of Chap. 5, stochastic hyperbolic models could also exhibit various bifurcations when we vary model parameters. These bifurcations could represent transitions between two different deterministic-types of patterns, or transitions between deterministic and random patterns (e.g., from a travelling pulse for low noise, to a chaotic zigzag for medium noise, and a stationary pulse for high noise; see Fig. 5.26a).

Similar to the deterministic case, the stochastic bifurcation theory focuses on qualitative changes in parametrised classes of stochastic dynamical systems [57]. While the bifurcation theory for deterministic PDE systems is well developed [3, 17], the field of stochastic bifurcations for stochastic PDEs is still not fully developed [58], and to our knowledge it was never applied to the very few stochastic hyperbolic/kinetic models derived to investigate pattern formation in animal aggregations. For this reason, we will not detail here the basic concepts of stochastic bifurcation theory, but we refer the reader to the books by Arnold [59] and Blömker [58] (which introduce and develop the concepts of bifurcation theory for stochastic ODEs and PDEs). However, for the completeness of our discussion on bifurcations, in the following we discuss briefly two approaches used to describe bifurcations in the context of random dynamical systems. As noted in [58], these two approaches sometimes can give completely different results.

- A *D-bifurcation* or *dynamical bifurcation* is characterised by changes in the structure of the random attractor (e.g., as shown by the sign changes in the Lyapunov exponents for the random dynamical system);
- A *P-bifurcation* or *phenomenological bifurcation* is characterised by changes in the density function for stationary measures associated with the random dynamical system.

These two concepts can be used to describe the classical types of bifurcations that can appear in a stochastic context (e.g., stochastic pitchfork, stochastic transcritical, saddle node, or Hopf bifurcations) [57, 60, 61].

Similar to the case of deterministic PDEs, one could approximate the stochastic PDEs with amplitude equations for the dominant modes, which could be then used to investigate the impact of noise on the dynamics of the system near points of changes in stability [58]. However, one needs to emphasise that, as for deterministic hyperbolic PDEs, spectral gap properties might impact the possibility of deriving such amplitude equations through random centre manifold reductions.

8.8 Bifurcation and Symmetry Theory in the Context of Hyperbolic/Kinetic Models

To conclude this chapter, we need to review the application of the previous notions of stability and bifurcation theory to the kinetic and hyperbolic models discussed in the previous chapters. In this context, we note that the calculation of the steady states and their stability (as well as the existence of different classical and weak solutions) are relatively common approaches taken when investigating the patterns generated by different models [14, 27, 29, 44, 62–69]. However, the analytical investigation of the branches bifurcating at different points where spatially homogeneous and heterogeneous solutions loose their stability is still an open problem for the vast majority of models discussed throughout this monograph, as well as for many other models in the literature (which were not even mentioned here, due to the limited space and purpose of this study). As we have seen above, one of the main reasons for this lack of results is the applicability of the Centre Manifold Theorem for different classes of hyperbolic systems. While it was shown in [30] that this theorem holds for the nonlocal 1D hyperbolic systems introduced in Chap. 5, its applicability to the majority of all other hyperbolic/kinetic models discussed here is still an open problem.

Similarly, the impact of various symmetries on model dynamics has been mainly investigated for nonlocal hyperbolic models [27–30]. As seen above in our discussion on the symmetries of Boltzmann and Fokker-Planck models, many other models in the literature do exhibit similar $\mathbf{O}(2)$ and $\mathbf{SO}(2)$ symmetry, which impacts the types of patterns one expects to see [3]. However, this investigation is still an open problem in the context of the models for collective behaviours in biology. Equally an open problem is the understanding of the similar-looking patterns displayed by some deterministic hyperbolic models with symmetry and the corresponding stochastic models without symmetry (see Fig. 5.26).

The impact of this lack of results on the understanding of the bifurcating dynamics of the models summarised in this monograph will become more evident in the next Chapter, as Table 9.1 will show that only the nonlocal hyperbolic systems discussed in Chap. 5 have been observed to exhibit a large variety of spatial and spatio-temporal patterns (some of which were identified through the rigorous investigation of the solution branches bifurcating near codim-1 and codim-2 points). However, it is expected that many other hyperbolic and kinetic classes of models could exhibit equally interesting spatial and spatio-temporal patterns and bifurcations. The identification of these potential patterns can only be done by combining analytical approaches with intensive numerical simulations (which still needs to be performed for the majority of models discussed throughout this monograph).

References

1. W. Holmes, Bull. Math. Biol. **76**(1), 157 (2014)
2. R. Hoyle, *Pattern Formation. An Introduction to Methods* (Cambridge University Press, Cambridge, 2006)
3. M. Golubitsky, I. Stewart, *The Symmetry Perspective: From Equilibrium to Chaos in Phase Space and Physical Space* (Birkhäuser, Basel, 2002)
4. P. Chossat, R. Lauterbach, *Methods in Equivariant Bifurcations and Dynamical Systems* (World Scientific Publishing, Singapore, 2000)
5. M. Haragus, G. Iooss, *Local Bifurcations, Center Manifolds, and Normal Forms in Infinite-Dimensional Dynamical Systems* (Springer, London, 2010)
6. Y. Kuznetsov, *Elements of Applied Bifurcation Theory*, 2nd edn. (Springer, New York, 2000)
7. S. Strogatz, *Nonlinear Dynamics and Chaos* (Westview Press, Boulder, 1994)
8. J.D. Murray, *Mathematical Biology* (Springer, New York, 1989)
9. L. Perko, *Differential Equations and Dynamical Systems* (Springer, New York, 2000)
10. C. Chicone, *Ordinary Differential Equations with Applications* (Springer, New York, 1999)
11. R. Eftimie, G. de Vries, M.A. Lewis, Proc. Natl. Acad. Sci. USA **104**(17), 6974 (2007)
12. T. Kolokolnikov, M. Ward, J. Wei, Discr. Contin. Dyn. Syst. Ser. B **19**(5), 1373 (2014)
13. T. Kolokolnikov, W. Sun, M. Ward, J. Wei, SIAM J. Appl. Dyn. Syst. **5**(2), 313 (2006)
14. R. Eftimie, G. de Vries, M.A. Lewis, F. Lutscher, Bull. Math. Biol. **69**(5), 1537 (2007)
15. F. Lutscher, J. Math. Biol. **45**, 234 (2002)
16. H. Poincaré, Acta Math. **7**, 259 (1885)
17. M. Golubitsky, I. Stewart, D.G. Schaeffer, *Singularities and Groups in Bifurcation Theory. Volume II* (Springer, New York, 1988)
18. R. Seydel, *Practical Bifurcation and Stability Analysis* (Springer, New York, 2009)
19. J.C. Robinson, *Infinite-Dimensional Dynamical Systems* (Cambridge University Press, Cambridge, 2001)
20. L. Evans, *Partial Differential Equations* (American Mathematical Society, Providence, 1997)
21. H. Knobloch, B. Aulbach, in *Equadiff5, Proceedings of the Fifth G. Teubner Verlagsgesellschaft*, ed. by M. Greguš (Teubner, Leipzig, 1982), pp. 179–189
22. E. Altshuler, O. Ramos, Y.N. ez, J. Fernández, A. Batista-Leyva, C. Noda, Am. Nat. **166**(6), 643 (2005)
23. G. Li, D. Huan, B. Roehner, Y. Xu, L. Zeng, Z. Di, Z. Han, PLoS One **9**(12), e114517 (2014)
24. Y.K. Chung, C.C. Lin, PLoS One **12**(3), e0173642 (2017)
25. Q. Ji, C. Xin, S. Tang, J. Huang, Phys. A Stat. Mech. Appl. **492**, 941 (2018)
26. N. Zabzina, A. Dussutour, R. Mann, D. Sumpter, S. Nicolis, PLoS Comput. Biol. **10**(12), e1003960 (2014)
27. P.L. Buono, R. Eftimie, Math. Models Methods Appl. Sci. **24**(2), 327–357 (2014)
28. P.L. Buono, R. Eftimie, SIAM J. Appl. Dyn. Sys. **13**(4), 1542 (2014)
29. P.L. Buono, R. Eftimie, J. Math. Biol. **71**(4), 847 (2014)
30. P.L. Buono, R. Eftimie, *Mathematical Sciences with Multidisciplinary Applications*. Springer Proceedings in Mathematics & Statistics, vol. 157 (Springer, Cham, 2016), pp. 29–59
31. J. Massot, R. Bacis, J. Math. Phys. **17**, 1392 (1976)
32. M. Makai, Transp. Theory Stat. Phys. **15**(3), 249 (1984)
33. A. Bobylev, G. Caraffini, G. Spiga, J. Math. Phys. **37**(6), 2787 (1996)
34. S. Takata, J. Stat. Phys. **136**(4), 751 (2009)
35. Y. Grigoriev, S. Meleshko, N. Ibragimov, V. Kovalev, *Symmetries of Integro-Differential Equations: With Applications in Mechanics and Plasma Physics* (Springer, Dordrecht, 2010)
36. O. Ilyin, Theor. Math. Phys. **186**(2), 183 (2016)
37. A.W.H. Mochaki, J.M. Manale, On Modified Symmetries for the Boltzmann Equation. Proceedings **2**, 7 (2018)
38. I. An, S. Chen, H.Y. Guo, Phys. A Stat. Mech. Appl. **128**(3), 520 (1984)
39. C. Sastri, K. Dunn, J. Math. Phys. **26**, 3042 (1985)

40. P. Rudra, J. Phys. A Math. Gen. **23**(10), 1663 (1990)
41. R. Kozlov, J. Eng. Math. **82**(1), 39 (2013)
42. D. Métivier, Kinetic models, from Kuramoto to Vlasov: bifurcations and experimental analysis of a magneto-optical trap, Université Côte d'Azur (2017) (English)
43. C. Kubrusly, Bull. Belg. Math. Soc. Simon Stevin **15**(1), 153 (2008)
44. R. Eftimie, G. de Vries, M. Lewis, J. Math. Biol. **59**, 37 (2009)
45. I. Kmit, L. Recke, J. Math. Anal. Appl. **335**, 355 (2007)
46. A. Vanderbauwhede, *Lyapunov–Schmidt Method for Dynamical Systems* (Springer, New York, 2011), pp. 937–952
47. A. Bressan, D. Serre, M. Williams, K. Zumbrun, *Hyperbolic Systems of Balance Laws* (Springer, Berlin, 2007)
48. A. Mielke, J. Differ. Equ. **65**, 68 (1986)
49. A. Mielke, Math. Meth. Appl. Sci. **10**, 51 (1988)
50. A. Vanderbauwhede, in *Dynamics in Infinite Dimensional Systems*, ed. by S.N. Chow, J. Hale (Springer, Berlin , 1987), pp. 409–420
51. A. Vanderbauwhede, G. Iooss, in *Dynamics Reported*, vol. 1, ed. by C. Jones, U. Kirchgraber, H. Walter (Springer, Berlin, 1992), pp. 125–163
52. M. Lichtner, Proc. Am. Math. Soc. **136**(6), 2091 (2008)
53. M. Renardy, Z. Angew. Math. Phys. **45**(6), 854 (1994)
54. M. Renardy, Proc. R. Soc. Edin. Sect. A **122**(3–4), 363 (1992)
55. M. Lichtner, M. Radziunas, L. Recke, Math. Methods Appl. Sci. **30**, 931 (2007)
56. W. Liu, M. Oh, in *Infinite Dimensional Dynamical Systems*, ed. by J. Mallet-Paret, J. Wu, H. Zhu (Springer, New York, 2013), pp. 169–183
57. L. Arnold, P. Boxler, *Diffusion Processes and Related Problems in Analysis, Volume II*. Progress in Probability, vol. 27 (Birkhäuser, Boston, 1992), pp. 241–255
58. D. Blömker, *Amplitude Equations for Stochastic Partial Differential Equations* (World Scientific Publishing, Singapore, 2007)
59. L. Arnold, *Random Dynamical Systems* (Springer, Berlin, 1998)
60. H. Crauel, P. Imkeller, M. Steinkamp, *Stochastic Dynamics* (Springer, New York, 1999), pp. 27–47
61. C. Kuehn, Physica D **240**(12), 1020 (2011)
62. K. Lika, T. Hallam, J. Math. Biol. **38**, 346 (1999)
63. C.M. Topaz, A.L. Bertozzi, M.A. Lewis, Bull. Math. Bio. **68**, 1601 (2006)
64. K. Fellner, G. Raoul, Math. Comput. Model. **53**, 1436 (2011)
65. K. Fellner, G. Raoul, Math. Models Methods Appl. Sci. **20**, 2267 (2010)
66. G. Raoul, Differ. Integr. Equ. **25**(5/6), 417 (2012)
67. D. Balagué, J. Carrillo, T. Laurent, G. Raoul, Phys. D Nonlinear Phenom. **260**, 5 (2013)
68. P.H. Chavanis, Phys. A Stat. Mech. Appl. **387**, 5716 (2008)
69. F. Lutscher, A. Stevens, J. Nonlinear Sci. **12**, 619 (2002)